Available online at www.sciencedirect.com
ScienceDirect
Geochimica et Cosmochimica Acta 74 (2010) 7362–7388
Geochimica et Cosmochimica Acta
www.elsevier.com/locate/gca

On the origin of impact glass in the Apollo 16 regolith

Randy L. Korotev [a,c,*], Ryan A. Zeigler [a,c], Christine Floss [b,c]

[a] Department of Earth and Planetary Sciences, Washington University, Campus Box 1169, Saint Louis, MO 63130, USA
[b] Laboratory for Space Sciences and Department of Physics, Washington University, Campus Box 1105, Saint Louis, MO 63130, USA
[c] McDonnell Center for the Space Sciences, Washington University, Campus Box 1169, Saint Louis, MO 63130, USA

Received 5 February 2010; accepted in revised form 15 September 2010; available online 26 September 2010

Abstract

This study addresses the issue of what fraction of the impact glass in the regolith of a lunar landing site derives from local impacts (those within a few kilometers of the site) as opposed to distant impacts (10 or more kilometers away). Among 10,323 fragments from the 64–210-μm grain-size fraction of three Apollo 16 regolith samples, 14% are impact glasses, that is, fragments consisting wholly or largely of glass produced in a crater-forming impact. Another 16% are agglutinates formed by impacts of micrometeorites into regolith. We analyzed the glass in 1559 fragments for major- and minor-element concentrations by electron probe microanalysis and a subset of 112 of the fragments that are homogeneous impact glasses for trace elements by secondary ion mass spectrometry. Of the impact glasses, 75% are substantially different in composition from either the Apollo 16 regolith or any mixture of rocks of which the regolith is mainly composed. About 40% of the impact glasses are richer in Fe, Mg, and Ti, as well as K, P, and Sm, than are common rocks of the feldspathic highlands. These glasses must originate from craters in maria or the Procellarum KREEP Terrane. Of the feldspathic impact glasses, some are substantially more magnesian (greater MgO/FeO) or have substantially lower concentrations of incompatible elements than the regolith of the Apollo 16 site. Many of these, however, are in the range of feldspathic lunar meteorites, most of which derive from points in the feldspathic highlands distant from the Procellarum KREEP Terrane. These observations indicate that a significant proportion of the impact glass in the Apollo 16 regolith is from craters occurring 100 km or more from the landing site. In contrast, the composition of glass in agglutinates, on average, is similar to the composition of the Apollo 16 regolith, consistent with local origin.

1. INTRODUCTION

Impact-produced glass, which occurs in the lunar regolith in a variety of textures and morphologies (spheroidal, ropy, vesicular, shards, and coatings), was the subject of immediate interest when the first lunar samples were studied in laboratories (Chao et al., 1970, 1972; Apollo Soil Survey, 1971; Glass, 1971; Prinz et al., 1971; Reid et al., 1972a,b,c). The interest was undoubtedly sparked in part by its novelty, as glass of impact origin is not a component of most terrestrial regoliths. Although there have been many studies of lunar impact glass, the knowledge base is much broader now for interpretation of the glass data than it was in the 1970s, particularly with respect to relating glass compositions to rock compositions and viewing the data in a global context in light of new data obtained from remote sensing and lunar meteorites.

The primary goal of this study is to put quantitative limits on the proportion of impact glass occurring in "soil" (<1-mm fines) at a given location that was produced in distant impacts (tens of kilometers or more) relative to the amount of impact glass produced by local impacts (e.g., the scale of sampling over the Apollo 16 landing site, about 8 km). Previous studies have not addressed this issue in a systematic or quantitative way, although several studies have laid the groundwork (Delano et al., 1981, 2007; Simon

* Corresponding author. Address: Department of Earth and Planetary Sciences, Washington University, Campus Box 1169, Saint Louis, MO 63130, USA. Tel.: +1 314 935 5637.
E-mail address: Korotev@wustl.edu (R.L. Korotev).

0016-7037/$ - see front matter © 2010 Elsevier Ltd. All rights reserved.
doi:10.1016/j.gca.2010.09.020

et al., 1989; Delano, 1991; Wentworth et al., 1994; Zellner et al., 2002, 2009; Zeigler et al., 2006). Such information can aid in interpreting samples and data from future robotic missions (Delano et al., 1981). Samplers deployed on some such missions will have limited mobility and will collect samples of small mass, by Apollo standards. Some of the material will be regolith fines that will undoubtedly contain impact glass. From our Apollo experience, we would expect some of that glass to be exotic to the site and thus to provide information about locations not sampled directly. We expect that the results of our study will also be useful for interpreting data on ages of lunar impact glasses (e.g., Delano et al., 2007; Zellner et al., 2009).

Our study focuses on regolith from the Apollo 16 site because most of the lunar surface consists of regolith developed from feldspathic rocks and the Apollo 16 mission was the only Apollo mission to land in the FHT (Feldspathic Highlands Terrane; Jolliff et al., 2000) at a point distant from the mafic maria. The Apollo 16 site also has a special distinction that makes it ideal for our goal. Although a majority of the rocks in the regolith are characteristic of the FHT in being feldspathic and having low concentrations of incompatible elements, a significant fraction are impact-melt breccias that are mafic (basaltic, noritic, or troctolitic) and moderately rich in K, REE (rare earth elements), P, and other elements associated with KREEP (Korotev, 1997; Zeigler et al., 2006). Most of the KREEP-bearing breccias likely originate from in or near the PKT (Procellarum KREEP Terrane; Jolliff et al., 2000) to the northwest of the Apollo 16 site (Korotev, 2000). As a consequence of the site's location near the PKT and the Imbrium basin, the Apollo 16 regolith is richer in KREEP-related elements (e.g., Warren, 1989) than is regolith from most places in the feldspathic highlands (Fig. 1). Previous studies have shown that most of the impact glass in the Apollo 16 regolith is feldspathic in composition, although some is more mafic (e.g., Ridley et al., 1973; Zeigler et al., 2006; Delano et al., 2007). Our working assumption is that if a fragment of feldspathic impact glass has concentrations of incompatible elements in the range of the Apollo 16 soil, then it was likely produced in or near the Apollo 16 site. If concentrations of incompatible elements are substantially lower or greater, then the glass likely formed elsewhere. A problem in applying this approach is that compositions of impact glass have been determined almost exclusively by EPMA (electron probe microanalysis). Although this technique determines the concentrations of two KREEP elements, K and P, both elements can be fractionally vaporized from hot impact melt (Delano et al., 1981), so low concentrations of K and P in impact glass do not necessarily reflect the composition of the target nor imply origin distant from the Apollo 16 site.

For the study described here, we analyzed glassy fragments from the Apollo 16 regolith by EPMA for major elements and a selected subset of these by SIMS (secondary ion mass spectrometry) for trace elements, some of which (e.g., the REE) are refractory and not subject to loss during impact heating. Most of the fragments that we studied are glasses produced in crater-forming impacts, which we desig-

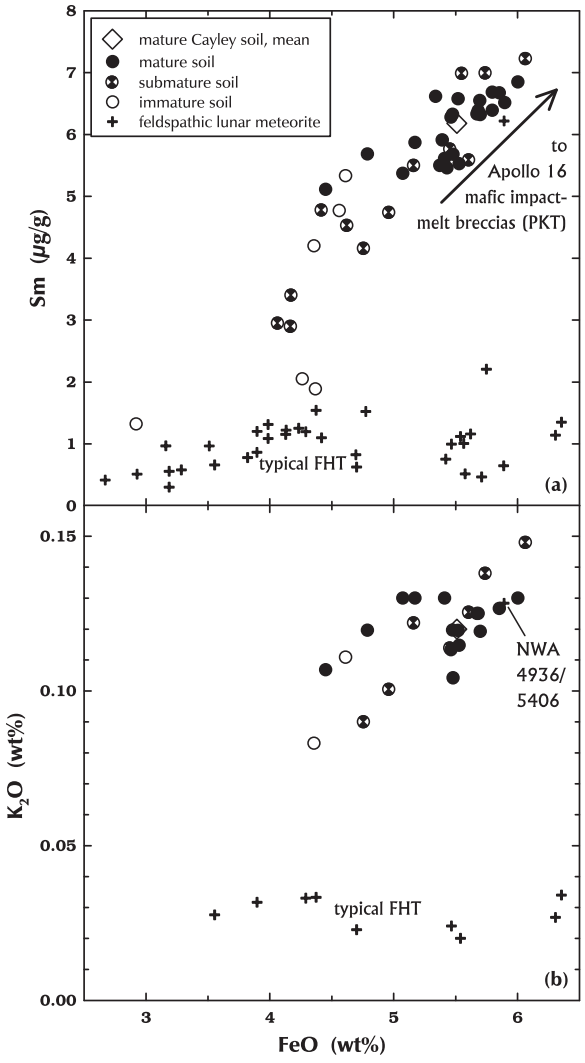

Fig. 1. Comparison of compositions of Apollo 16 regolith samples to feldspathic lunar meteorites. Each circular point represents an Apollo 16 surface or trench soil sample (6xxx1; $N = 42$) keyed by maturity (Morris et al., 1978). The diagonal square represents the mean of the mature samples, the "mature Cayley soils" model component of Korotev et al. (1997). Submature and immature soils are mixtures of mature soil and feldspathic ejecta from recent craters that have had little surface exposure (Korotev, 1996, 1997). The mature soils, in turn are mixtures, made mainly at the time of basin formation, of two components, (1) typical FeO-, Sm-, and K-poor feldspathic material of the Feldspathic Highlands Terrane (65%; see text), represented here by the numerous feldspathic lunar meteorites and (2) FeO-, Sm-, and K-rich, mafic impact-melt breccias that likely originate from in or near the Procellarum KREEP Terrane (29%; the 6% is mainly post-basin mare basalt and glass). In (b), K_2O (and MgO; Fig. 21) data are not available for all Apollo 16 soil samples. Except for paired stones NWA 4936 and NWA 5406, only meteorites from Antarctica are plotted because meteorites from hot deserts are commonly enriched in K from terrestrial alteration. NWA 4936/5406 is the meteorite (+) plotting with the soils. It is the only lunar meteorite likely to have originated near the Apollo 16 site (Korotev et al., 2009). *Sources of data:* Korotev (1997), Korotev et al. (2006, 2009), and references cited therein.

nate "impact glass" to be consistent with previous studies. To our knowledge there have been only three previous studies of lunar impact glass by SIMS, those of Meyer (1978), Simon et al. (1989), and Zeigler et al. (2006). For comparison, we have also analyzed some glass from agglutinates, which form by the impact of micrometeorites into regolith (McKay et al., 1991). Agglutinates are identified by the highly vesicular and clast-laden nature of the impact glass. The vesicles form during release of solar-wind-implanted gases during impact melting. Agglutinates are also characterized by the presence of nanophase iron metal in the glass (Morris, 1976; Basu et al., 1996; Basu, 2005). Although literally also "impact glass," we will refer to glass from agglutinates as "agglutinitic glass," following Hu and Taylor (1977) and Pieters and Taylor (2003), and exclude it from the "impact glass" category.

2. SAMPLES AND ANALYSIS

We sieved 0.21–0.25-g subsamples of Apollo 16 regolith samples 61221, 61241, and 68841 using nylon-mesh sieves and acetone. Mesh sizes were 500, 210, 105, and 64 μm. We prepared grain mounts of the 64–105 and 105–210 μm grain-size fractions and had them thin sectioned in the curatorial laboratory at NASA Johnson Space Center. The samples were selected to represent immature (61121, I_s/FeO = 9.2), submature (61241, I_s/FeO = 47), and mature (68841, I_s/FeO = 70) regoliths (Morris, 1978). Each grain mount also contained three fragments of glass prepared by melting the JB-1 (basalt) geochemical reference standard (Kurasawa, 1968).

In each of the six grain mounts, we imaged a contiguous area encompassing at least 1300 particles (Table 1) in transmitted, cross-polarized, and reflected light as well as with high-resolution BSE (backscattered-electron) image mosaics (Fig. 2) and elemental X-ray maps. These images were coregistered and used in concert to identify and classify each individual particle. The first order categorization was to identify each particle as a lithic (rock) fragment, an agglutinate, or impact glass. Many characteristics were considered when classifying particles, however. Agglutinates were most easily identified in reflected light (vesicular nature) and BSE images (schlieren), whereas impact glasses were most easily identified in cross-polarized light (isotropic). The impact glasses were then further subdivided into a variety of classes based on their textures and clast-loads: clean, mostly-clean, cryptocrystalline, vitrophyre, ropy, and clast-laden (see Section 3.1 for definitions).

We analyzed the glass fragments for major- and minor-elements (Si, Ti, Al, Cr, Fe, Mn, Mg, Ca, Na, K, P) by wavelength dispersive spectroscopy using the JEOL 8200 Superprobe at Washington University. Analyses were done at an accelerating voltage of 15 keV, beam current of 25 nA, and spot sizes ranging from 10 to 20 μm. Data were reduced using a combination of mineral and glass standards (Zeigler et al., 2006). We obtained EMPA data for a total of 1534 glass fragments, with multiple analyses on a single glass averaged together (total number of analyses was ~3000). The number of glass fragments analyzed is less than the number of glass fragments identified, 2067 ($N = 6 + 1431 + 630$; Table 1), because for many of the clast-laden fragments, there were no 10-μm regions of clast-free glass. Also, in a few cases poor sum-of-oxide totals were caused by poor carbon coatings; these data were discarded.

For a subset of 112 impact glasses from the three soil samples we determined trace element concentrations by SIMS, using the modified Cameca ims 3f ion microprobe at Washington University. Details of the experimental technique can be found in Zinner and Crozaz (1986a) and data reduction procedures follow those outlined in Floss (2000). All analyses were made using an O^- primary ion beam and energy filtering at low mass resolution to remove complex molecular interferences. Corrections for simple molecular interferences not removed by energy filtering are made by deconvolving the mass spectrum in the mass regions for K–Ca–Sc–Ti, Rb–Sr–Y–Zr, and Ba–REEs. Trace element concentrations are obtained by normalization of the ion signals to the SiO_2 contents of the glasses, using sensitivity factors reported in Zinner and Crozaz (1986b) and Hsu (1995). On the basis of SIMS data for the JB-1 glass, which was analyzed together with the lunar glasses and which we have analyzed by INAA (instrumental neutron activation analysis; e.g., Korotev et al., 2009) on 15 occasions, REE concentrations were further normalized by a factors ranging from 1.009 (Lu) to 1.407 (Eu). This procedure is necessary because we compare SIMS data for glasses directly to data for bulk samples (soils, rocks) determined by INAA. Potassium data were multiplied by a factor of 1.223 to match, on average, data obtained on the same glasses by EPMA.

Using the same conditions described above, we analyzed the glass in agglutinates in the 61241 grain mounts by EPMA in an effort to understand the variability in agglutinitic glass composition, both within a single agglutinate particle and among different agglutinates found within a single soil (Table 2). To determine the average composition of agglutinitic glass, we analyzed 62 analytical spots within the glassy areas of 37 different agglutinate grains. We used a 10-μm beam size for the 64–105-μm grain mount and a 20-μm beam size for the 105–210-μm grain mount. For each agglutinate grain, we analyzed 1–4 spots based on the size of the grain and amount of clast-free glass. To estimate the variability agglutinitic glass composition, we also analyzed, using a 2-μm electron beam size, an average of 12 spots within the same broad-beam (10-μm and 20-μm) analytical spots in 34 of the 37 agglutinates for a total of 418 2-μm analyses.

In order to determine the degree of crystallinity in some optically isotropic grains that had compositions corresponding to pyroxene, olivine, and silica, we did spectroscopic analysis using a Hololab 5000-532 Raman spectrometer (Kaiser Optical Systems, Inc.). The 532 nm line of a frequency-doubled Nd:YAG solid state laser was used as the excitation source. All analyses were done using a 20× long-working distance objective (NA 0.4), which condenses laser beam into a spot of 6 μm diameter on the sample, with an average power of 11 mW. This objective also collects the back-scattering Raman photons from the sample. These photons were sent through a multimode optical fiber to Raman spectrograph. A volume holographic grating

Table 1
Results of modal analysis: number (*N*) and percent of fragments (%).

Grain-size fraction	61221				61241			
	105–210 μm		64–105 μm		105–210 μm		64–105 μm	
	N	%	*N*	%	*N*	%	*N*	%
Lithic	1464	77.1	1025	74.0	1053	69.6	1576	57.0
Pyroclastic	1	0.05	0	0.00	1	0.07	3	0.11
Agglutinate	76	4.0	55	4.0	142	9.4	489	17.7
Impact glass	*359*	*18.9*	*305*	*22.0*	*317*	*21.0*	*695*	*25.2*
Clean	52	2.7	56	4.0	130	8.6	206	7.5
Clast laden and ropy	52	2.7	27	1.9	45	3.0	133	4.8
Vitrophyric	24	1.3	17	1.2	38	2.5	86	3.1
Cryptocrystalline	18	0.9	26	1.9	23	1.5	142	5.1
HASP	7	0.37	2	0.14	3	0.20	11	0.40
Mineral	*206*	*10.8*	*177*	*12.8*	*78*	*5.2*	*117*	*4.2*
Maskelynite	204	10.7	164	11.8	77	5.1	115	4.2
Pyroxene and olivine	0	0.0	10	0.7	1	0.07	0	0.0
Silica	2	0.11	4	0.29	0	0.00	2	0.07
$\sum$	1900	100.0	1386	100.0	1513	100.0	2763	100.0
% IG/(IG + Aggl.)		66.8		69.9		62.7		54.2
I_s/FeO	9.2				47			
% agglutinates		6.3			27.1			

	68841				All		EPMA	
	105–210 μm		64–105 μm		64–210 μm		64–210 μm	
	N	%	*N*	%	*N*	%	*N*	%
Lithic	782	55.7	708	52.1	6608	64.0	0	0.0
Pyroclastic glass	1	0.07	0	0.0	6	0.06	6	0.4
Agglutinate	444	31.6	442	32.5	1648	16.0	37	2.4
Impact glass	*177*	*2.6*	*208*	*15.3*	*1431*	*13.9*	*888*	*57.0*
Clean	38	2.7	70	5.2	552	5.3	356	22.8
Clast laden and ropy	39	2.8	53	3.9	349	3.4	195	12.5
Vitrophyric	46	3.3	36	2.7	247	2.4	179	11.5
Cryptocrystalline	19	1.4	12	0.9	240	2.3	115	7.4
HASP	9	0.64	11	0.81	43	0.42	43	2.8
Mineral	*26*	*1.9*	*26*	*1.9*	*630*	*6.1*	*628*	*40.3*
Maskelynite	24	1.7	23	1.7	607	5.9	606	38.9
Pyroxene and olivine	2	0.14	3	0.22	16	0.15	16	1.03
Silica	0	0.0	0	0.00	8	0.08	6	0.38
$\sum$	1404	100.0	1358	100.0	10324	100.0	1559	100.0
% IG/(IG + Aggl.)		25.4		29.2		46.5		
I_s/FeO	70							
% agglutinates		n.a.						

Values in italics are the sums of the indented items in underlying rows and are not included in the sum ($\sum$). The EPMA columns indicate the number of each fragment type analyzed by electron probe microanalysis. I_s/FeO data for <250 μm grain-size fraction from Morris (1978). The rows "% IG/(IG + Aggl.)" presents the % of agglutinate and impact glass fragments that are impact glasses. Data for "% agglutinates" are from Heiken et al. (1973) based on data for 300 fragments in the 90–150 μm grain-size fraction.

spectrometer disperses the collected Raman photons into a Raman Stokes shift range of 100–4300 cm^{-1} relative to the 532-nm laser line, with a spectral resolution of 4–5 cm^{-1}. Multiple Raman spectra were collected from each of 11 grains in the 64–105-μm grain-size fraction of sample 61221 with total acquisition time of 20 s. See Freeman et al. (2008) for more analytical details.

Finally, we report here concentrations of FeO and Sm that we obtained by neutron activation analysis during the studies of Korotev (1991) and Zeigler et al. (2006) but which we did not specifically report in those papers. The samples are individual impact-glass spherules separated from the Apollo 16 regolith. Seven (all <1 μg in mass) are from the deep drill core (60002–60006 sections). Four are from the 1–2 mm grain-size fraction of sample 66042 (5–11 mg each) and the remaining seven are from the 2–4 mm grain-size fractions of samples 60043, 66083, and 69943 (9–35 mg each).

3. RESULTS

3.1. Classification

Most of the 10,323 particles examined, 64%, are largely-crystalline lithic fragments (Fig. 3). Another 16% are agglutinates (Table 1, Fig. 3). The percentage of agglutinates

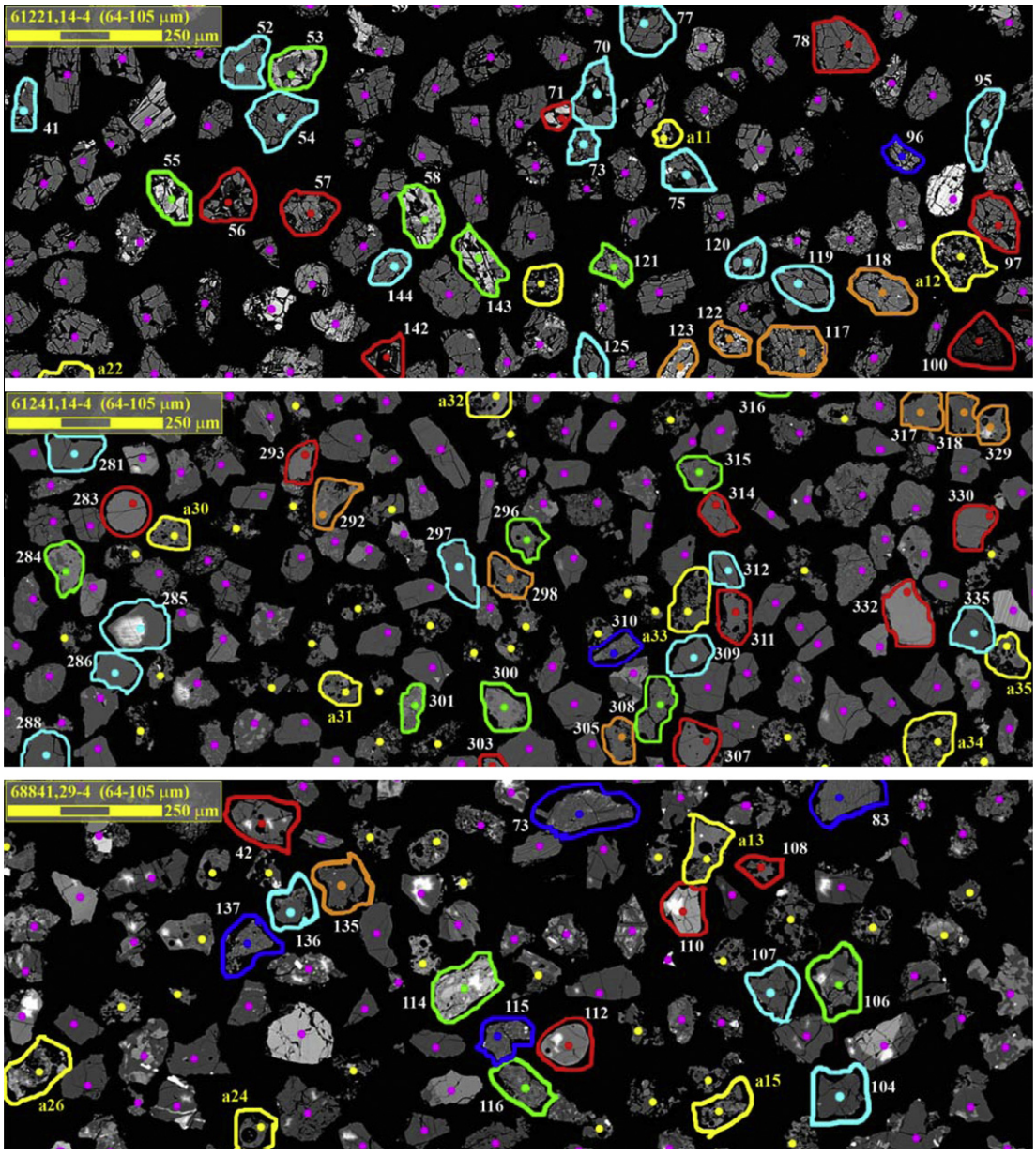

Fig. 2. Backscattered-electron image of portions of grain mounts (64–105-µm grain size fractions) of 61221 (immature), 61241 (submature), and 68841 (mature). The glass in the encircled grains was analyzed by electron probe microanalysis for the data of Tables 2 and 3; the other fragments were categorized for lithologic type by their texture in images such as this (Table 1). *Pink dot:* non-glass (not analyzed), *yellow:* agglutinate (not always analyzed), *red:* clean or mostly clean (includes high-alumina, silica poor or HASP), *green:* clast-laden, *orange:* cryptocrystalline, *dark blue:* vitrophyre, *cyan:* maskelynite.

varies widely from sample to sample, however. In immature soil 61121 only 4% of the fragments are agglutinates, whereas in the mature soil 66841, 32% of the fragments are agglutinates. This difference is consistent with quantitative measures of soil maturity (McKay et al., 1974).

A large number ($N = 630$) of the grains that we identified as glass based on optical microscopy have compositions of corresponding to pure minerals, almost always plagioclase (Fig. 4). We double checked each glassy fragment with a mineral composition to be certain that it was optically isotropic in crossed-polarized light. The glass grains with plagioclase compositions are presumably all maskelynite. They are most abundant in the most immature sample, 61121, where they account for 11% of the fragments (Table 1). Most maskelynite fragments are fractured and a few contain mafic clasts, metal grains, or even vesicles. A few of the fragments that we identified as glass have compositions consistent with silica ($N = 8$), pyroxene (15), or olivine (1). Most (14) of these other "mineral glasses" also are from sample 61221. The olivine glass has Fo_{80} composition, similar to the single olivine glass in the study of Delano et al. (2007), Fo_{77}. Both low- and high-Ca pyroxene glasses were

Table 2
Mean EPMA data for composition of agglutinitic glass in sample 61241.

	SiO_2	TiO_2	Al_2O_3	Cr_2O_3	FeO	MnO	MgO	CaO	Na_2O	K_2O	P_2O_5	Sum	FeO+MgO	Mg'	N
2 μm	44.1	0.53	27.6	0.11	5.10	0.07	5.95	15.40	0.44	0.11	0.09	99.3	11.0	66.9	418
s.d.	2.1	0.24	3.0	0.05	1.56	0.03	1.96	1.24	0.13	0.10	0.21	0.6	3.3	4.4	
10 μm	44.0	0.48	27.7	0.10	5.03	0.06	5.86	15.15	0.40	0.10	0.07	99.0	10.9	67.2	26
s.d.	0.9	0.18	2.5	0.05	1.47	0.02	1.87	1.23	0.11	0.08	0.04	0.3	3.2	3.4	
20 μm	44.3	0.59	27.3	0.11	5.39	0.07	6.20	15.19	0.41	0.13	0.08	99.8	11.6	66.7	36
s.d.	1.4	0.26	2.6	0.03	1.43	0.02	2.31	1.22	0.09	0.05	0.06	0.6	3.4	4.3	
95%	0.5	0.09	0.9	0.01	0.48	0.01	0.78	0.41	0.03	0.02	0.02	0.2	1.2	1.5	
Station 1 soil	45.0	0.57	27.0	0.105	5.22	0.064	5.86	15.4	0.48	0.114	0.115	99.3	11.1	66.7	–
95%	0.3	0.05	0.6	0.010	0.39	0.003	0.46	0.3	0.01	0.015	0.008	0.4	0.9	0.8	

Oxide values in mass percent, Mg' in mole percent MgO/(MgO + FeO). N is the number of analytical spots. For the agglutinitic glasses, the table presents means and standard deviations (s.d.) for N analyses of three different spot diameters. For the 20-μm data, the 95% confidence limit is also presented. The agglutinate data are compared with the mean composition of all seven surface and trench soils collected from station 1. The soil data from Bansal et al. (1972), Finkelman et al. (1975), Haskin et al. (1973), Korotev (1982, 1997), McKay et al. (1986), Müller (1975), Rose et al. (1973), Taylor et al. (1973), and Wänke et al. (1973).

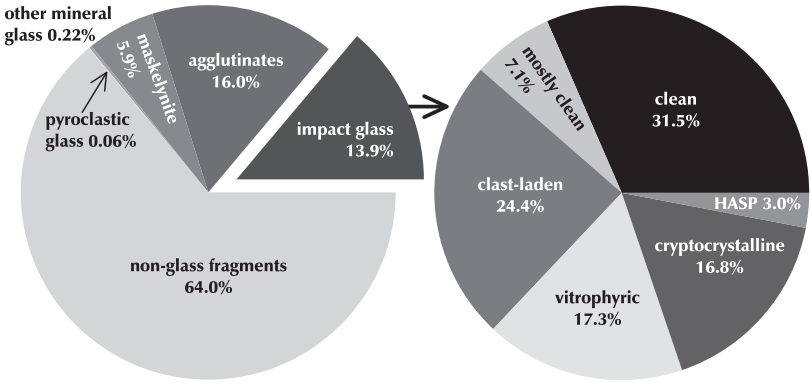

Fig. 3. Modal proportions of glass fragment types in the 10,323 fragments of the study.

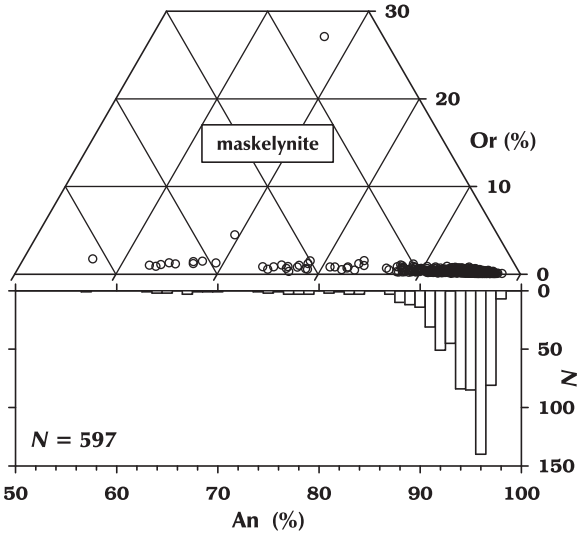

Fig. 4. Composition of maskelynite fragments plotted on a portion of the anorthite–orthoclase–albite ternary diagram (top) and histogram of plagioclase composition, as percent anorthite (bottom).

identified (sometimes with exsolution preserved). The Mg' (mole percent MgO/[MgO + FeO]) of the pyroxene glass ranges from 34 to 78 with a mean of 67. Despite their isotropic nature in visible light, Raman spectroscopy shows that the olivine and pyroxene fragments are not truly glass. All the analyzed fragments have Raman vibrational stretches characteristic of the minerals. Data for the silica glass is more ambiguous. We did not observe any peaks for quartz or its polymorphs in the four grains examined. The spectra were dominated by high background from the mounting epoxy, however. Finally, one of the clast-laden glasses (below) has 18.2 wt% P_2O_5 and 2.56 wt% K_2O, leading to 15% normative K feldspar and 40% normative apatite. Although curiosities, we do not discuss these mineral glasses further. On the basis of morphology, texture, and composition, six (0.06%) of the fragments are not impact glass but are of volcanic origin and are identical to the green picritic glass beads found in other Apollo 16 soil samples (Delano, 1975; Zeigler et al., 2006) (Fig. 5). All other glasses of basaltic composition are of impact origin as they have vesicles, dust coatings, clasts, or irregular shapes, unlike these pyroclastic glasses.

On the basis of morphology, texture (mainly the absence of vesicles), and composition, 13.9% of the glasses are distinct from agglutinates and mineral glass. As noted above, we designate this subset of glasses as "impact glass" to distinguish it from agglutinitic glass. Prior to chemical

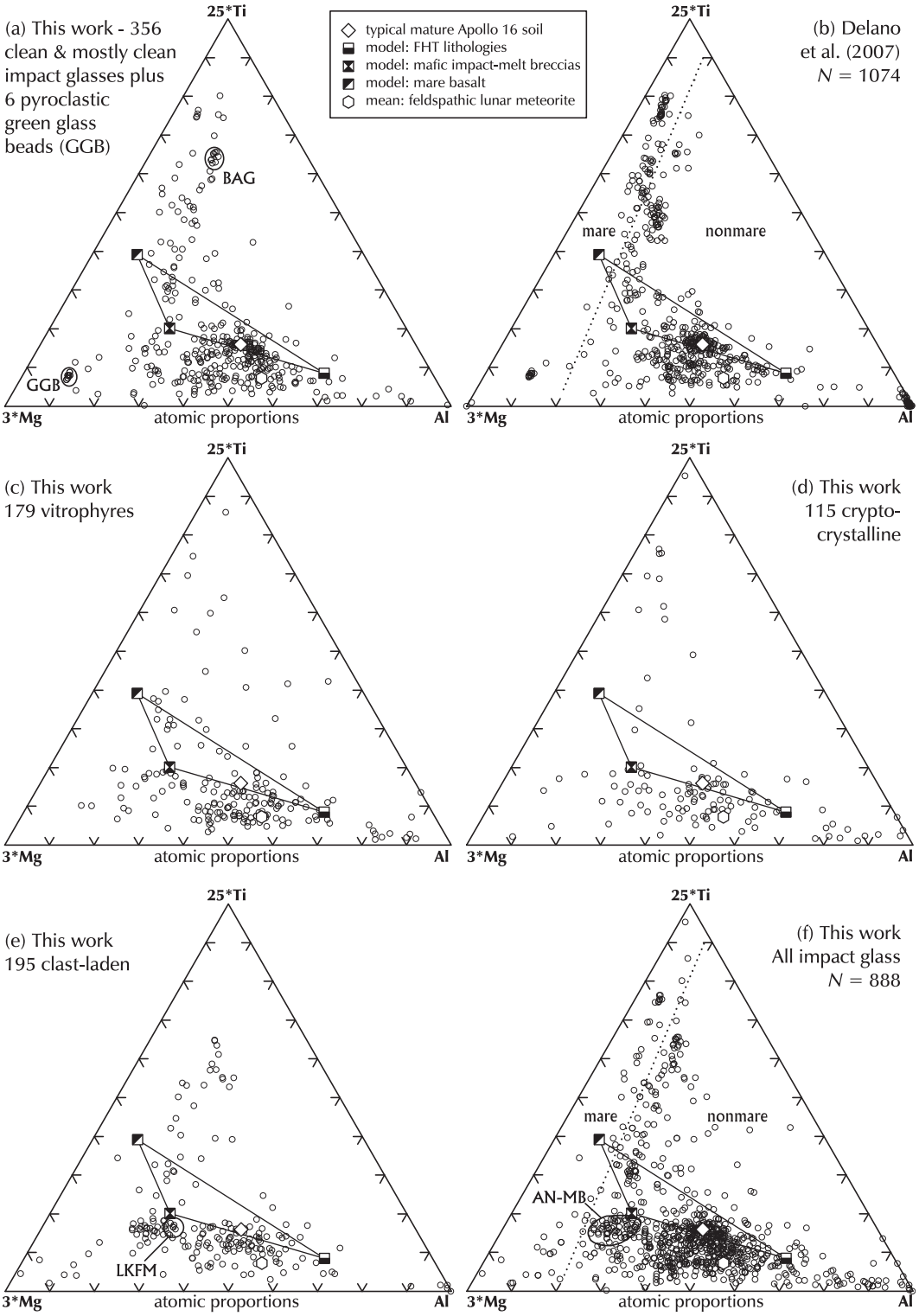

Fig. 5. Ternary diagrams, using three nonvolatile elements (after Delano et al. (2007)), comparing compositions of glasses of this study with those of Delano et al. (2007). The squares at the apices of the inner triangle represent the three main model components that account for the composition of Apollo 16 soils (Korotev, 1997). The mean composition of the soil is represented by the diagonal square. The hexagon represents the mean composition of 20 feldspathic lunar meteorites (Table 3). (a) The field for the green glass beads (GGB) and basaltic andesite glasses (BAG) of Zeigler et al. (2006) are indicated. (b) The dotted line represents the approximate boundary between mare and nonmare compositions (Delano et al., 2007). (e) The mean composition of Apollo 16 low-K Fra Mauro glass of Ridley et al. (1973) is shown. (f) The field for the AN–MB (anorthositic norite–mare basalt) glasses is shown.

analysis, we subdivided the impact glasses into five textural categories: clean, mostly clean, cryptocrystalline, vitrophyric, and clast-laden, largely following the naming conventions of Houck (1982a,b) (Table 1, Fig. 3). Clean glass is defined as a glass fragment lacking schlieren or other compositional nonuniformity and without mineral grains or clasts (<1-μm FeNi metal grains or a small amount of soil stuck to the exterior of the grain is permissible). "Mostly clean" glasses also lack compositional zoning, but do contain a few small clasts (the clasts are not included in the analyses). Because of our selection criteria, at most only a small fraction of our clean and mostly clean glasses can have originated from agglutinates, as the presence of schlieren would disqualify them as "clean." Cryptocrystalline glasses have small amounts of compositional nonuniformity, typically manifested as amorphous areas that appear to be slightly brighter or darker in BSE images. Vitrophyric glasses have numerous small crystals that have quenched from the glass. These differ from clast-laden glasses, which have areas of glass (typically homogeneous), but which contain numerous mineral or (more rarely) lithic clasts. Given that they are polymict, the clast-laden glasses fall into the "(Impact) glass or glassy melt breccia" category of Stöffler et al. (1980) for nomenclature of lunar highlands rocks.

A small fraction, 3.0%, of the impact glasses are of the high-alumina, silica-poor composition known as HASP (Naney et al., 1976; Delano et al., 1981). These glasses have lost volatile elements relative to refractory elements as a result of impact vaporization (Fig. 6). Compositionally, as the name indicates, HASP glasses are easy to recognize on the basis of their high Al_2O_3 and low SiO_2 concentrations (Fig. 7), which leads, normatively, to positive olivine and negative pyroxene (Wentworth and McKay, 1988). HASP glasses occur among each of the textural types.

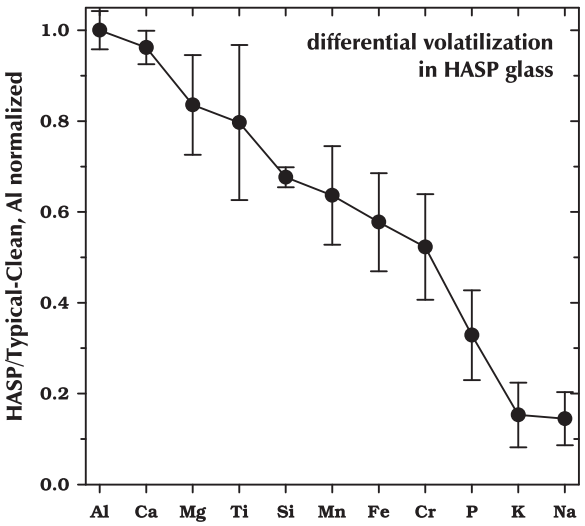

Fig. 6. Mean relative depletion, relative to typical clean glasses, in major elements in 43 HASP (high-alumina, silica-poor) glasses. Error bars are 95% confidence limits. The data are qualitatively consistent with the expectation based on vapor pressures of oxides (Delano et al., 1981) and, to a lesser extent, Rayleigh fractionation (Boschelli and McKay, 1987).

However, we have separated out the HASP glasses from the various textural classes and have not included them in means calculated for the textural types in Table 3. In effect, we treat them as a sixth textural type (e.g., Figs. 7 and 8), although the classification is based on composition. All of the recognized HASP glasses appear to derive from the feldspathic highlands (Figs. 7 and 8). We note, moreover, that our HASP suite would include the "silica-poor gabbroic anorthosite glass" of Wentworth and McKay (1988).

3.2. Composition overview and data presentation

On a plot of Al_2O_3 concentration against FeO plus MgO concentration, most glasses of this study have compositions lying along a mixing line between plagioclase and pyroxene (Fig. 8). All lunar regolith samples (Lucey et al., 2006) and most lunar rocks (e.g., lunar meteorites; Korotev, 2005) plot along the same trend. The anticorrelation is a closure effect associated with the simple mineralogy of the lunar crust. Lunar rocks are dominated by plagioclase and pyroxene, with lesser amounts of olivine and ilmenite. Thus, the glasses are mainly impact mixtures of these four minerals. As the proportion of Fe- and Mg-bearing minerals increase, the proportion of plagioclase and Al_2O_3 necessarily decreases. Some glasses (basaltic andesite and high-K_2O, high-P_2O_5 to be discussed later) plot off the trend because they are unusual in containing normative silica (~7%). The concentration of FeO + MgO of olivine is greater than that of pyroxene. Thus, at low Al_2O_3, points falling to the high FeO + MgO side of the trend, e.g., those representing the pyroclastic green-glass beads, have higher-than-average normative olivine/pyroxene. HASP glasses plot off the trend because they have lost silica. Typical plagioclase of the lunar highlands is of An_{96} composition (e.g., Fig. 4), which has 36.0 wt% Al_2O_3. As the anorthite proportion decreases, SiO_2 increases (Fig. 7) and Al_2O_3 decreases (Fig. 8). In Fig. 8, the intercept of the line is 38.6 wt% Al_2O_3, greater than the stoichiometric concentration of alumina in pure anorthite. This discrepancy suggests that many of the aluminous glasses not definitively identified as HASP in the figure have, in fact, lost some silica, which leads to an increase in the alumina concentration. In the same type of plot, but for bulk regolith samples, the intercept is 36.4 wt% Al_2O_3 (Fig. 2.12b of Lucey et al. (2006)).

We and others (Table 4 of Korotev (1997)) have shown that the composition of the Apollo 16 regolith can be modeled as a mixture of three main classes of materials: (1) Al-rich material from the feldspathic highlands, (2) moderately mafic (noritic and troctolitic) material, rich in incompatible elements such as K, P, and Sm, that likely originates in or near the Procellarum KREEP Terrane, and (3) mafic (basaltic) material from the maria. Crystalline forms of the feldspathic materials are mainly breccias ranging in composition from anorthosite to anorthositic norite and troctolite, but also include shocked, but unbrecciated, anorthosite with >90% plagioclase. The mafic impact-melt breccias contribute 80–85% of the incompatible elements that occur in the Apollo 16 regolith and are, in effect, the main carriers of KREEP signature at this site. In the model of Korotev (1997) for the <1-mm fines of Apollo 16, the

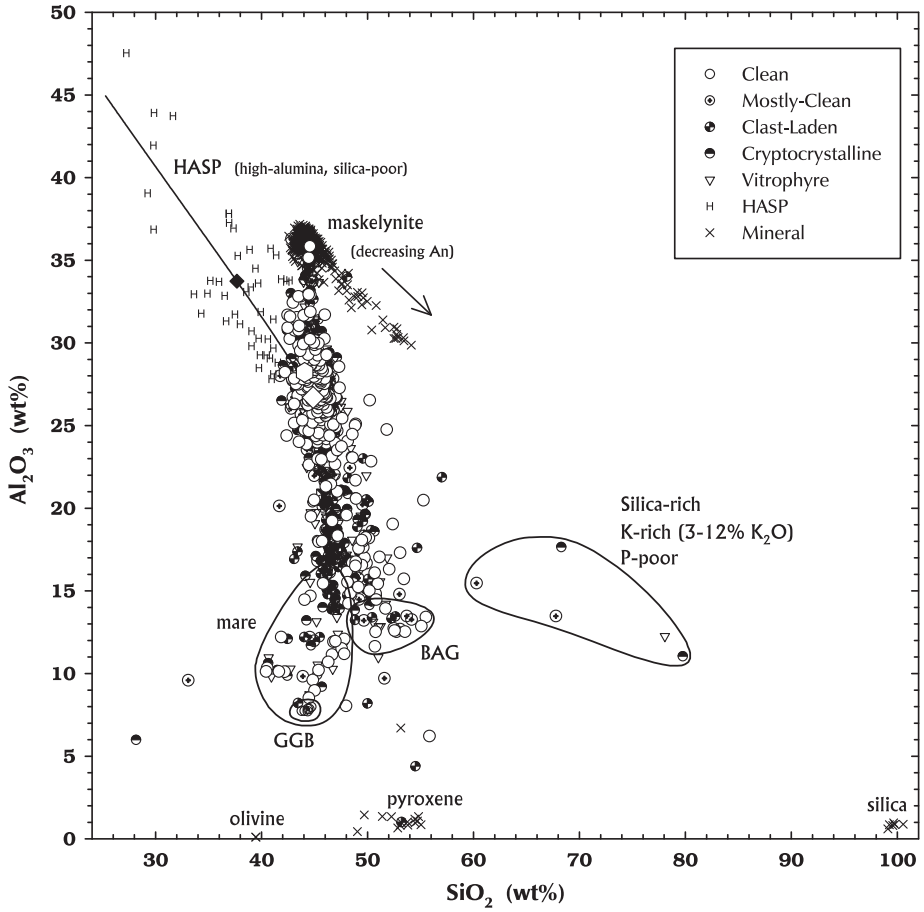

Fig. 7. Variation of concentrations of Al_2O_3 with SiO_2 in the glasses (EPMA glasses of Table 1, excluding the agglutinates; $N = 1522$). See Fig. 8 for key to other symbols. The line in the HASP (high-alumina, silica-poor) field represents the path of the residual glass composition with increasing fractional vaporization assuming that all HASP glass derives from melting of material of typical, mature soil composition (unfilled diagonal square; Table 3), there is no loss of Al_2O_3, and the path of residual glass composition passes through the point corresponding to the mean composition of the HASP glasses (filled diagonal square).

proportions of the three components are 65% material of the Feldspathic Highlands Terrane (columns 4 + 5 of Table 7 of Korotev (1997)), 29% mafic impact-melt breccias (column 2), and 6% mare material (column 6). Because one of our goals is to relate glass compositions to rock types, we plot the compositions of these three model components in a number of the figures for reference (e.g., Figs. 5, 9 and 10). In several figures, the range of compositions of the Apollo 16 mafic impact-melt breccias is also shown (defined by groups 1M, 1F, 2DB, and 2Mo of Korotev (1997, 2000)). Because Apollo 16 mafic melt breccias have moderately low concentrations of incompatible elements compared to those of sites closer to the Imbrium basin, we also plot the "high-K KREEP" composition of Warren (1989), which is based mainly on melt breccias from Apollo 14. Also shown for reference on many plots is the "mature Cayley soil" composition of Korotev (1997). This composition represents the common soil at the surface of the site. Immature soils composed mainly of material excavated from North Ray Crater as well as some units of immature soil found in cores tend to be more feldspathic and have lower concentrations of incompatible elements (Korotev, 1991, 1997; Fig. 1). Finally, the mean composition of 20 feldspathic lunar meteorites that are regolith breccias or fragmental breccias (Table 3) is shown to represent the near surface of the feldspathic highlands at points distant from the Procellarum KREEP Terrane (Korotev et al., 2003, 2006). This composition is that which we would expect for glass produced by impacts forming kilometer-sized craters in regions of typical feldspathic highlands distant from the Procellarum KREEP Terrane.

3.3. Clean impact glasses

The compositional range and average compositions of the clean and mostly-clean glasses are indistinguishable from each other (Fig. 8). Thus, in subsequent discussion, "clean" refers to both the clean and mostly clean glasses of Table 1. The mean composition and distribution of clean glasses in this study (Fig. 5a) are largely similar to those of the glasses in the study of Delano et al. (2007), which considered only clean glass (Fig. 5b). The main difference is that there is a greater proportion of glasses of basaltic (high-Ti) composition in the study of Delano et al. (2007)

Table 3
Mean compositions of textural and compositional glass groups.

	note	*N*	SiO_2	TiO_2	Al_2O_3	Cr_2O_3	FeO	MnO	MgO	CaO	Na_2O	K_2O	P_2O_5	Sum	Mg'	FeO+MgO
Mature soil	1	–	45.3	0.60	26.7	0.113	5.50	0.070	6.14	15.29	0.457	0.119	0.122	100.0	66.6	11.6
±			0.3	0.03	0.3	0.006	0.25	0.003	0.24	0.14	0.007	0.007	0.007	0.4	0.6	0.5
Impact glass	2	888	45.7	0.88	24.2	0.153	6.86	0.098	7.23	14.05	0.45	0.166	0.119	99.85	65.3	14.1
Felds. meteorites	3	–	44.2	0.23	28.3	0.098	4.5	0.067	5.2	16.1	0.35	0.028	0.026	99.7	66.6	9.7
			0.3	0.03	0.8	0.014	0.5	0.008	0.7	0.6	0.04	0.004	0.004	0.24	1.7	1.2
Clean, all	4	356	46.1	0.90	23.8	0.147	6.8	0.096	7.2	13.9	0.42	0.15	0.07	99.64	66.3	14.0
±			0.3	0.13	0.6	0.012	0.4	0.006	0.3	0.3	0.03	0.03	0.10	0.07	1.1	0.6
Clean, typical	5	232	45.15	0.42	27.4	0.100	4.65	0.066	6.27	15.35	0.39	0.059	0.038	99.86	70.1	10.9
±			0.17	0.02	0.3	0.006	0.16	0.003	0.23	0.14	0.03	0.005	0.004	0.07	0.7	0.3
Clast-laden	6	195	46.5	0.92	21.7	0.196	8.5	0.121	7.9	13.0	0.55	0.19	0.19	99.87	61.8	16.4
±			0.3	0.14	0.9	0.019	0.6	0.009	0.5	0.4	0.06	0.04	0.05	0.10	1.4	1.0
Cryptocrystalline	7	115	45.6	1.15	24.8	0.140	6.1	0.087	7.1	14.1	0.50	0.25	0.08	100.01	66.1	13.2
±			0.8	0.56	1.2	0.023	0.8	0.012	0.9	0.6	0.06	0.23	0.02	0.12	2.4	1.4
Vitrophyre	8	179	45.8	0.75	24.8	0.149	6.6	0.096	6.9	14.4	0.46	0.16	0.08	100.13	65.0	13.4
±			0.4	0.18	0.9	0.020	0.6	0.009	0.5	0.4	0.04	0.08	0.02	0.10	1.7	1.0
Maskelynite	9	606	44.66	0.031	35.89	0.008	0.126	0.009	0.056	18.67	0.71	0.049	0.016	100.23	42.7	0.182
±			0.12	0.002	0.09	0.001	0.005	0.001	0.004	0.09	0.05	0.015	0.001	0.05	1.2	0.008
HASP	10	43	37.6	0.41	33.7	0.064	3.3	0.052	6.5	18.2	0.07	0.011	0.015	99.95	77.4	9.8
±			1.2	0.09	1.4	0.014	0.6	0.009	0.8	0.7	0.03	0.005	0.004	0.19	3.9	1.1
Basaltic andesite	11	19	51.9	3.48	13.3	0.14	12.8	0.172	5.00	9.5	1.00	0.77	0.73	98.8	41.1	17.8
±			0.8	0.12	0.4	0.02	0.3	0.014	0.18	0.5	0.13	0.15	0.26	0.3	1.3	0.3
AN–MB, low-Fe	12	69	46.2	0.53	22.3	0.25	8.4	0.12	8.5	13.35	0.38	0.10	0.05	100.2	64.4	17.0
AN–MB, high-Fe	12	69	46.8	0.76	13.2	0.50	15.2	0.24	11.7	10.42	0.12	0.06	0.04	99.1	57.9	27.0
High K and P	13	16	48.9	2.9	15.1	0.16	11.9	0.16	6.2	10.5	0.99	0.95	1.15	98.9	47.6	18.0
±			0.7	0.4	1.6	0.05	1.8	0.03	1.2	0.5	0.13	0.35	0.34	0.3	6.0	1.8
Silica-rich	14	5	71.	0.3	14.	0.02	2.5	0.03	1.6	2.7	1.4	6.0	0.04	99.4	24.	4.0
±			10.	0.5	3.	0.03	3.8	0.04	2.9	3.7	0.8	4.7	0.04	1.2	34.	6.6
Pyroclastic GGB	15	6	44.3	0.37	7.81	0.42	21.53	0.260	16.22	8.27	0.16	0.014	0.021	99.4	57.3	37.8
±			0.3	0.04	0.11	0.04	0.18	0.012	0.18	0.13	0.05	0.015	0.007	0.4	0.3	0.3

All compositional values are in mass percent; uncertainties are 95% confidence limits. N = number of fragments. (1) "Mature Cayley soil," the typical soil of the Apollo 16 site (Table 1 of Korotev (1997), and data cited therein). (2) Simple mean of all impact glasses of Table 1, including HASP. (3) Mean composition of 20 feldspathic lunar meteorites (updated from Korotev et al. (2003, 2006)); data for CaO, Na_2O, K_2O, and P_2O_5 only from those eight meteorites from Antarctica. (4) Includes clean and mostly-clean glasses of Table 1. (5) Subset of (4) with compositions typical of the feldspathic highlands; see text. (6) Includes clast-laden and ropy glasses of Table 1. (7) Cryptocrystalline glasses and (8) vitrophyres of Table 1. (9) Isotropic glass of plagioclase composition. (10) High-Al, Si-poor glasses (after Naney et al. (1976)). (11) Glasses that fall in the compositional range of basaltic andesite glasses (BAG) of Zeigler et al. (2007). (12) The low-Fe and high-Fe end of regression lines of Fig. 16. (13) Glasses with >0.5% K_2O and >0.5% P_2O_5, excluding basaltic andesite glass and one highly anomalous glass with 18% P_2O_5 (Fig. 12). (14) Glasses with 60–80% SiO_2. (15) Pyroclastic "green glass beads" (Zeigler et al., 2007).

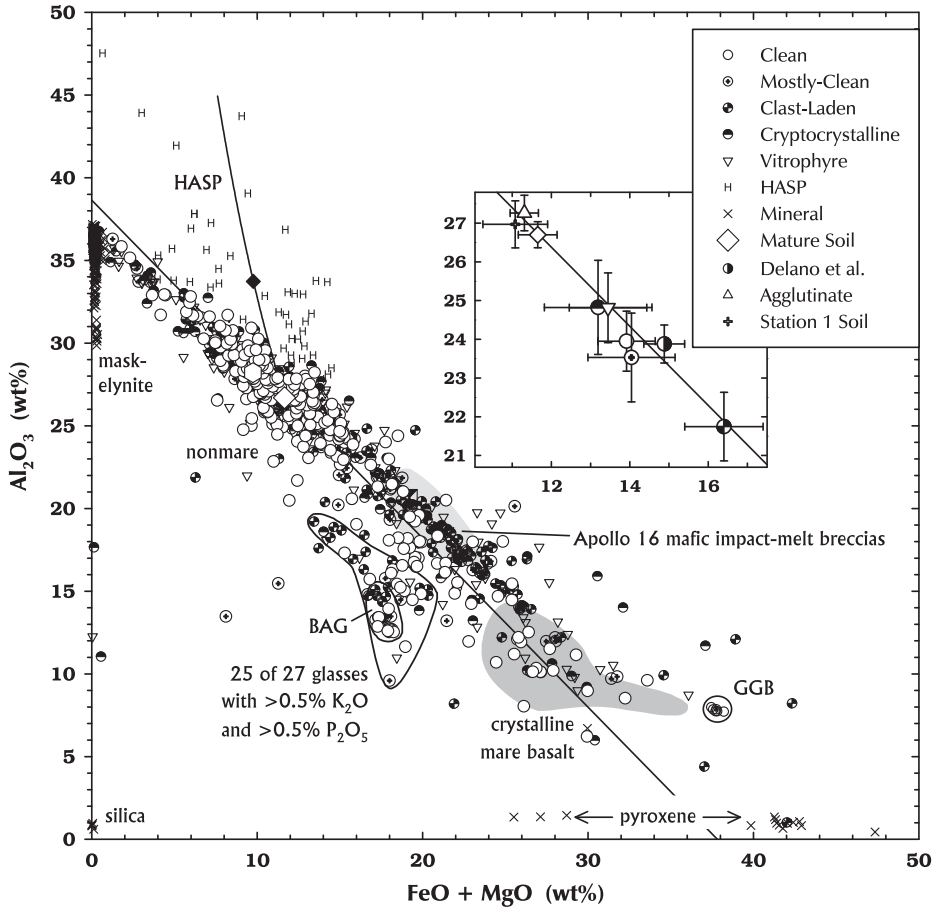

Fig. 8. Variation of concentrations of Al_2O_3 with FeO + MgO in impact glasses (EPMA glasses of Table 1, excluding the agglutinates and one fragment of olivine composition that plots off scale at 61% FeO + MgO and 0.11% Al_2O_3; $N = 1521$). The inset shows the mean composition of each of the textural types of glass and comparisons to the mean of the data of Delano et al. (2007), the mean of mature surface soils of Apollo 16 (Table 2), and mean composition of agglutinitic glasses (2-μm data) from station-1 sample 61241 (Table 2). For comparison to agglutinates, the + (upper left corner of inset) represents the mean composition of soils from station 1 (Fig. 17). All error bars represent 95% confidence limits. The diagonal line in both plots is a weighted least-squares regression to the data of the inset ($[Al_2O_3] = -1.0122 \cdot [FeO + MgO] + 38.64$). Glasses corresponding to the basaltic-andesite-glass (BAG) and green-glass-bead (GGB) compositional groups of Zeigler et al. (2006) are indicated as is the range of crystalline mare basalts (Apollo, Luna, meteorites). The line in the HASP field is the same as that of Fig. 7.

because their study included, along with more typical samples, some samples from the 64001 drive tube that are anomalously rich in mare-derived glass (Korotev et al., 1984). In total, 6.1% of the glasses of Delano et al. (2007) have >6 wt% TiO_2 whereas only 1.2% of the clean glasses of this study exceed 6 wt% TiO_2. (For the purpose of this comparison, we include the pyroclastic, mineral, and HASP glasses (Table 1) among the clean glasses, as did Delano et al. (2007).)

Most clean glass has a major-element composition similar to the Apollo 16 soil (Figs. 5, 9 and 10), although there are some important differences that we discuss below. In early studies in which compositional clusters were interpreted as representing prevalent rock types of the lunar crust, this composition was know as "highland basalt" or "anorthositic gabbro" (Reid et al., 1972a; Ridley et al., 1973; Wentworth and McKay, 1988; Zellner et al., 2009). A significant proportion, 35%, of the clean glasses are atypical of the feldspathic highlands, however, in being substantially more mafic or richer in incompatible elements. We define atypical as those glasses with any one of the following properties: (1) mafic composition, with >16 wt% FeO + MgO (Fig. 9), (2) Mg' less than 50 when both FeO and MgO exceed 2 wt% (Mg' is not determined precisely if FeO or MgO is <2 wt%) (Fig. 10), (3) TiO_2 exceeds 1 wt% (Fig. 9), or K_2O exceeds 0.2 wt% (Fig. 11). We choose 16 wt% FeO + MgO as the upper limit for typical highlands because there is a weak hiatus in the distribution of the glass data at this value (Figs. 8) and because any composition more mafic than this is normatively a norite, troctolite, gabbro, or basalt, not some variety of anorthositic rock (e.g., noritic anorthosite, anorthositic troctolite, etc.). Because of the high proportion of atypically mafic glasses, the mean composition of the clean glasses (67% normative feldspar) is distinctly more mafic than that of the typical soil at the surface of the site (74% normative plagioclase; mature Cayley soil of Korotev (1997)) (Fig. 8).

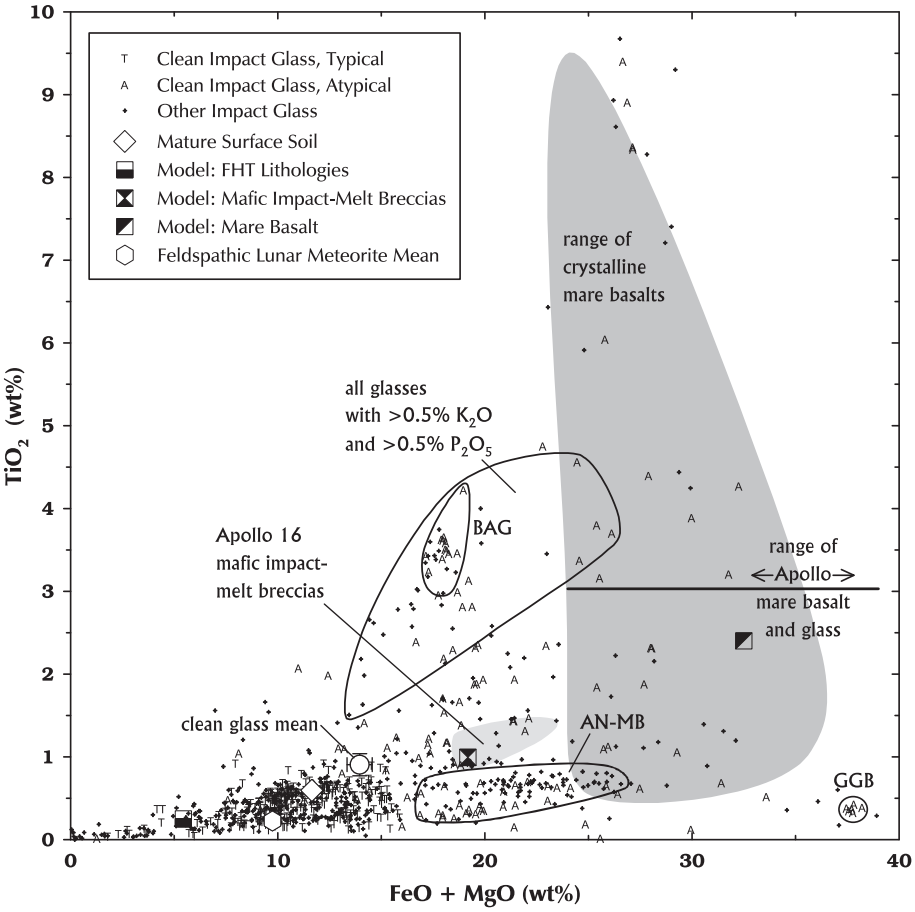

Fig. 9. Variation of TiO_2 with FeO + MgO in the typical (T) and atypical (A) clean glasses, as well as other (cryptocrystalline, vitrophyric, and clasts laden) textural types of impact glasses (+). The figure includes data for the analyzed (EPMA) "pyroclastic glass" (six spherules or broken spherules of green glass beads, GGB) and "impact glass" (but excluding HASP) of Table 1 for a total of 851 samples. "Typical" refers to typical of the feldspathic highlands, not necessarily the Apollo 16 site. The large squares represent the model components of Fig. 5 and Section 3.2 of the text. The range of groups 1M, 1F, 2DB, and 2Mo mafic impact-melt breccias of Apollo 16 (Korotev, 2000) is shown. Few glasses plot in this range. The horizontal line represents the range of FeO + MgO concentrations in mare basalts and volcanic glasses in the Apollo collection, 24–39%. The line is plotted at 3.03% TiO_2, the mean concentration of the 30 clean glasses with >24 wt% FeO + MgO, i.e., those atypical of the local soil and likely of mare origin. The field labeled BAG encloses glasses with the basaltic andesite glasses of Zeigler et al. (2006).

3.4. Other impact glass types, textural and compositional

Five glasses (2 mostly-clean, 2 cryptocrystalline, 1 clast-laden) have granite-like compositions in being rich in SiO_2 (60–80 wt%; Fig. 7) and K_2O (2.7–12.1 wt%; Fig. 12). The average composition (Table 3) corresponds to 26 wt% plagioclase (An_{53}), 35 wt% potassium feldspar, 8 wt% hypersthene (En_{56}), 30 wt% silica, and 0.7 wt% ilmenite and is similar to that of some Apollo felsites and granites, e.g., samples 73255,27 of Blanchard and Budahn (1979), 14321,1028 of Warren et al. (1983), and 12032,366-19 of Seddio et al. (2009). Glass of similar composition has been reported by Kempa and Papike (1980) in the Apollo 16 regolith.

We obtained SIMS data for 14 HASP glasses. In terms of refractory elements, most HASP glasses fall into two fields, a low-Sc/Al, low-Sm/Al field representing a feldspathic protolith and high-Sc/Al, high-Sm/Al field representing a more mafic and KREEP-bearing protolith (Fig. 13). Curiously, neither composition corresponds to either the feldspathic lunar meteorites or the Apollo 16 soil, although REE concentrations in the high-REE group are similar to those of the Apollo 16 soil (Fig. 14).

The cryptocrystalline and vitrophyric glasses have average compositions that are indistinguishable from each other (Table 3; Fig 8). Both are slightly more feldspathic (70% normative plagioclase) than the clean glasses (67%) because they contain a lower proportion of Fe-, Mg-, and Ti-rich rich glasses. In contrast, the clast-laden glass has a more mafic average composition (62% normative plagioclase) than the clean glass. This difference occurs mainly because a high proportion of the clast-laden glasses have mafic compositions (the AN–MB glasses discussed below) whereas only a small fraction of the clean glasses are of this composition (Fig. 5).

A number of the impact glasses are richer in Na_2O, K_2O, and P_2O_5 than any rock type at the Apollo 16 site (Figs. 11 and 12). Most of the K- and P-rich glasses are of the

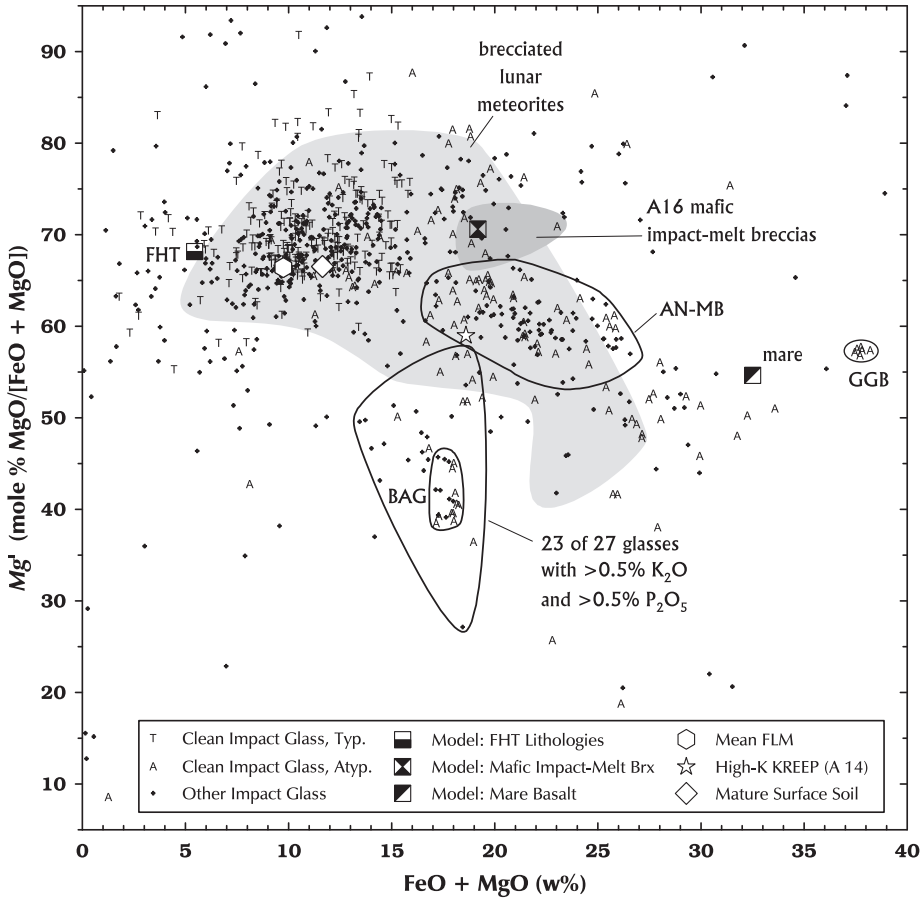

Fig. 10. Variation of magnesium number with FeO + MgO in clean (T, A), as well as other (cryptocrystalline, vitrophyric, and clasts laden) textural types of impact glasses (+). (Same sample set as Fig. 9.) We classify glasses with Mg' <50 as atypical (A) of the feldspathic highlands and likely of non-local origin. The hexagon represents the mean composition of the feldspathic lunar meteorites (Table 3) whereas the large light-gray field represents the range of all brecciated lunar meteorites. Similarly, the hour-glass square represents the model component of Apollo 16 mafic impact-melt breccias (Section 3.2 of the text) and the darker gray field represents the compositional range. *Acronyms:* FHT = Feldspathic Highlands Terrane; FLM = feldspathic lunar meteorite; BAG = basaltic andesite glass; GGB = green glass beads.

clast-laden variety. A number of the K- and P-rich glasses have concentrations of major elements that fall in the range of the basaltic andesite (BAG) glasses identified by Zeigler et al. (2006) (Table 3; Figs. 8–11). Other K- and P-rich glasses are qualitatively similar, with a few percent normative silica (Fig. 8) and low Mg' (Fig. 10) as well as moderately high concentrations of TiO_2 (Fig. 9).

Using the criteria of Papike et al. (1982), that is, CaO/Al_2O_3 >0.75 and FeO >13 wt%, 5.9% of the impact glasses are of mare affinity, that is, they were formed by impacts into a target dominated by mare basalt. We extend that definition to include seven glasses with <13 wt% FeO but with >16 wt% FeO + MgO, yielding 6.8% glasses of mare affinity (Fig. 15). This value is similar to that predicted on the basis of mass-balance constraints for total proportion of mare-derived material in the <1-mm fines (6.0 ± 1.4%, Korotev, 1997).

A number of our glasses form a compositional group that plot along a line between the most mafic of the typical highlands glasses (those of anorthositic norite composition, AN) and mare basalt (MB) on several of the compositional plots (most distinct in Fig. 15). We designate this group as the AN–MB glasses. These glasses are characterized by low TiO_2 (Fig. 9), low K_2O (Fig. 11), and increasing CaO/Al_2O_3 (Fig. 15) and decreasing Mg' (Fig. 10) with increasing mafic character. In Table 3, the average composition of the AN and MB ends of the inferred mixing trend are tabulated (calculated by regression; Fig. 16). If interpreted as mixtures of a nonmare anorthositic norite with ~17 wt% FeO + MgO and VLT (very-low-Ti) mare basalt (~1 wt% TiO_2, Fig. 9), then the proportion of basalt component ranges from zero for glasses at the AN end of the trend to 50–100% for glasses at the MB end, depending on the composition assumed for the basalt. (VLT basalts range from 25 to 34 wt% FeO + MgO.) Of the 69 glasses defining the AN–MB fields of Figs. 9, 11, 15, and 16, 12% are clean, 19% are cryptocrystalline or vitrophyric, and 70% are clast laden. Most (58%) come from sample 61241. The AN–MB glass has not been previously recognized as a compositional group. Glasses of this composition are included in the "ungrouped" glasses of Zeigler et al. (2006). None of the clean glasses of Delano et al. (2007) have concentrations

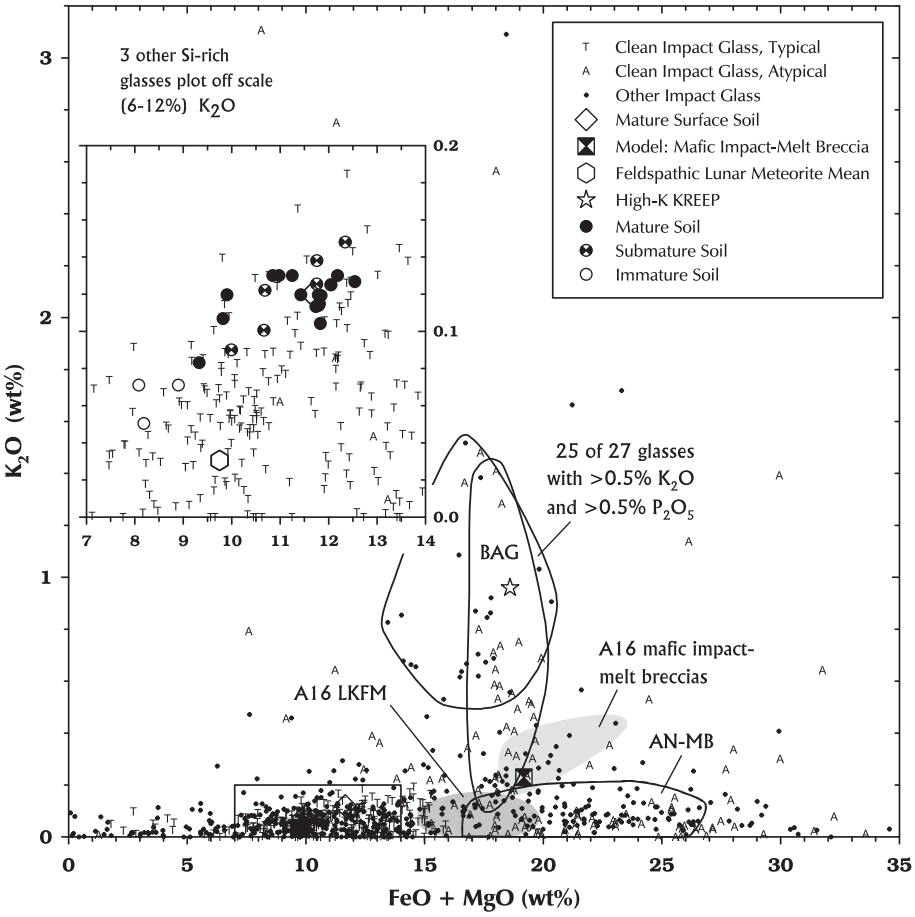

Fig. 11. Variation of K_2O (EMPA data) with FeO + MgO in impact glasses of this study (like Fig. 9). We classify all glasses with >0.2% K_2O as atypical of the feldspathic highlands and likely to be of non-local origin. The darker gray field represents the average composition of LKFM (low-K Fra Mauro basalt) glasses in Apollo 16 soil (±1 standard deviation ellipse) from Ridley et al. (1973). The inset compares the glass data with all samples of surface and trench soils from Apollo 16 for which there are FeO, MgO, and K_2O data (sources of Fig. 1).

of the five elements SiO_2, TiO_2, Al_2O_3, FeO, and MgO that all fall in the ranges defined by the AN and MB endmembers of Table 3, although two are close.

3.5. Agglutinitic glass

The range in composition of agglutinitic glass in station-1 sample 61241 is great (Fig. 17). In some agglutinates, the glass is moderately uniform in composition. For example, in agglutinate number 26, four 20-μm spots ranged from 9.2 to 10.1 wt% in FeO + MgO. In contrast, three 20-μm spots in agglutinate number 29 yielded 7.8, 16.9, and 20.3 wt% FeO + MgO. Most agglutinitic glasses plot along the plagioclase–pyroxene mixing trend of Fig. 8. Compositions range from that of pure plagioclase to that of norite. Much of the agglutinitic glass, however, has a composition in the range of the soil samples from station 1. For analysis of 2-μm-spots in agglutinitic glass, 43% of the spots have concentrations of both Al_2O_3 and FeO + MgO that were within two standard deviations of the mean concentrations in station-1 soils (based on data for soil samples 61141, 61161, 61181, 61221, 61241, 61281, and 61501). For the 10- and 20-μm spots, the proportion is 47%. Most of the outliers are simply more mafic or more feldspathic. The important observation is that the mean composition of agglutinitic glass in station-1 sample 61241 is essentially identical to the mean composition of the seven samples of surface and trench soil (<1-mm fines) from station 1 (Fig. 17). This observation is consistent with those of several previous studies (Marvin et al., 1971; Taylor et al., 1972; Gibbons et al., 1976; Hu and Taylor, 1977; Basu et al., 1996).

4. DISCUSSION

4.1. Granitic glass

The five silica-rich glasses of granitic composition (Fig. 7; Table 3) are a puzzle. If they are of impact origin, then they imply that somewhere on the Moon granite occurs on a size scale comparable to melt volume of an impact large enough to make glass. That need not be a large crater, but the fact that there are five such glasses indicates that the process that formed them is not uncommon.

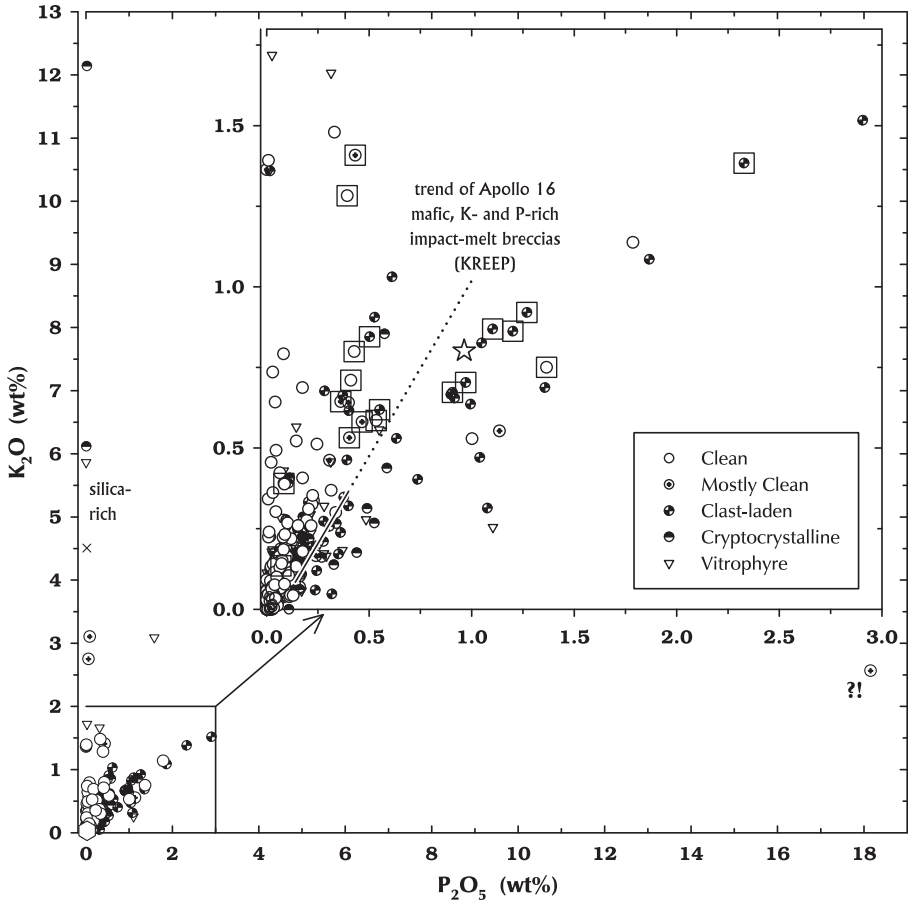

Fig. 12. K_2O/P_2O_5 in K- and P-rich basalts and impact-melt breccia (i.e., KREEP) of the Apollo collection is typically about 1.0 ± 0.4. For example, the mafic impact-melt breccias of the Apollo 16 site define the undashed portion of the line (K_2O/P_2O_5: 0.6–1.0) in the inset and the "av. high-K KREEP" of Warren (1989) is represented by the star (K_2O/P_2O_5: 1.2). Glasses of this study ($N = 845$; excludes HASP glasses) have highly variable K_2O/P_2O_5 compared to rocks, and concentrations of one or both elements exceed that of high-K KREEP in several samples. Of the 27 glasses with both >0.5 wt% K_2O and >0.5 wt% P_2O_5, all have >1.5 wt% TiO_2 (mean: 3.2 wt%, compared to 2.0 wt% in high-K KREEP) and most ($N = 18$) are clast-laden. Many (large squares) of the K- and P-rich glasses fall in the range of the "basaltic andesite glass" of Zeigler et al. (2007).

4.2. Fra Mauro basalt glasses

Glass with major-element compositions in the range of the Apollo mafic impact-melt breccias is common among impact glasses of the Apollo sites and has long known been known as "Fra Mauro basalt" glass because of its similarity in major-element composition to the regolith and melt rocks of Apollo 14 on the Fra Mauro formation. It has been recognized since the early 1970s that impact glasses with Fra Mauro basalt compositions (20 ± 3 wt% FeO + MgO) have highly variable concentrations of K_2O (e.g., Fig. 11). Thus, modifiers like low-K, intermediate-K, moderate-K, and high-K Fra Mauro basalt (Reid et al., 1972a,b; Vaniman and Papike, 1980) have been used to describe the glass compositions (see "Etymology and Evolution of LKFM" in Korotev (2000)). The acronym LKFM ("low-K Fra Mauro") was first applied by Ridley et al. (1973) to glasses in the Apollo 16 regolith with low K_2O concentrations (~0.08 wt%) and "aluminous basaltic" or "high alumina basalt" compositions (19–22 wt% Al_2O_3). Most actual rocks with Fra Mauro basalt compositions (normative norites or anorthositic norites) have greater concentrations of K and P than does LKFM glass, thus the source of LKFM glass has been enigmatic (Reid et al., 1977).

Although few of the glasses analyzed here fall in the field of the mafic impact-melt breccias that occur at the Apollo 16 site (Figs. 9–11), a number fall in the field of Apollo 16 LKFM glass as tabulated by Ridley et al. (1973). There is no hint of a compositional cluster of LKFM composition, however (Figs. 11 and 15). The most anorthositic of the AN–MB glasses falls in the Apollo 16 LKFM field but most of the AN–MB glasses are more mafic than any glass identified as LKFM from any site (Reid et al., 1977).

In addition to LKFM, Ridley et al. (1973) also recognized "high-K Fra Mauro basalt (KREEP)" glasses in the Apollo 16 regolith. The high-K Fra Mauro basalt glasses of Ridley et al. (1973) and some of the KREEP glasses of Wentworth and McKay (1988) are similar to the K- and P-rich glasses analyzed here. In detail, these glasses are

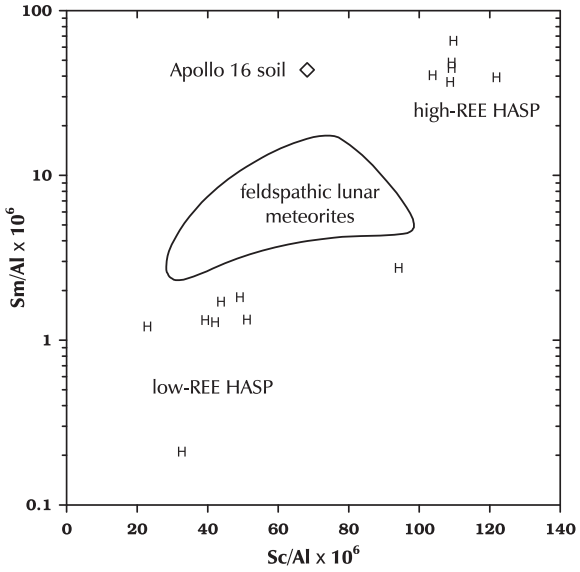

Fig. 13. Fourteen HASP (high-Al, Si-poor) glasses analyzed by secondary ion mass spectrometry fall into two compositional fields, one with low REE (Sm) and the other with moderately high REE. Neither composition matches either the Apollo 16 soil or the feldspathic lunar meteorites. The low-REE HASP glasses are more feldspathic ($39 \pm 5\%$ Al_2O_3 and $4.1 \pm 2.3\%$ MgO) than the high-REE HASP glasses ($31.3 \pm 1.2\%$ Al_2O_3 and $7.3 \pm 0.5\%$ MgO).

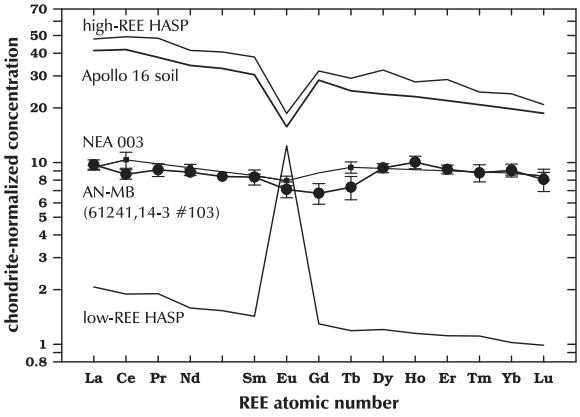

Fig. 14. Comparison of REE concentrations in the single AN–MB glass analyzed by secondary ion mass spectrometry and VLT (very-low-Ti) mare basalt of lunar meteorite Northeast Africa 003 analyzed by INAA (Haloda et al., 2009). Error bars represent 2-σ analytical uncertainties. Also shown are the REE patterns for the average of the two fields of HASP glasses of Fig. 13.

different from rocks (usually impact-melt breccias) of the high-K KREEP composition known from Apollo 12 and Apollo 14 rocks in that they are substantially richer in TiO_2 and have lower Mg' (Fig. 18). They are also variably depleted in K, Na, and P relative to REEs (Fig. 18), presumably because of fractional volatilization. The K- and P-rich glasses of Apollo 16 also differ from the type specimens of KREEP (Hubbard et al., 1971), the K- and P-rich glasses of Apollo 12. Again, the Apollo 16 glasses are richer in Ti and have lower Mg' (Fig. 18). Some HKFM glasses of Delano et al. (2007) have even greater TiO_2 and lower Mg' than those analyzed here. That study shows that at least some of the high-K impact glass in the Apollo 16 regolith date from the time of basin formation. It is tempting to hypothesize that LKFM glass is low in K as a result of volatilization from a target of medium- or high-K LKFM composition. However, K_2O/Sm is not systematically low, compared to KREEP, in glasses of LKFM major-element composition (Fig. 19), so there is no evidence for substantial loss of K from LKFM glasses.

It remains unclear the nature of the target rocks or regolith in the source region of impact glass of Fra Mauro basalt composition. Glasses of this composition at Apollo 16 are not consistent with common rocks (or mixtures thereof) that occur at the site, so we assume that they are all of nonlocal origin.

4.3. AN–MB glass

The previously unrecognized AN–MB glass is a significant component of the population of impact glass in the Apollo 16 regolith. Twenty-five percent of the impact glasses with >16 wt% FeO + MgO are of AN–MB composition. If the mafic component of the trends of Fig. 16 is, in fact, mare basalt, then we can estimate the composition of the basalt by extrapolation of the regression lines such as those of Fig. 16 into the range of mare basalt, i.e., 18–22 wt% FeO. For example, extrapolating to 18 wt% FeO yields 47.0 wt% SiO_2, 0.85 wt% TiO_2, 9.6 wt% Al_2O_3, 13.0 wt% MgO, and 9.2 wt% CaO. This composition is most similar to the VLT basalt of Apollo 17 (Wentworth et al., 1979; Lindstrom et al., 1994; Jolliff et al., 1996), the VLT olivine phyric basalt of paired lunar meteorites NWA (Northwest Africa) 2727 and NWA 3333 (Zeigler et al., 2007), and the mare basalt of lunar meteorite NEA (Northeast Africa) 003 (Haloda et al., 2009). In this example, the range of FeO concentrations of Fig. 16 corresponds to mixtures ranging from 0% to 73% mare basalt. An alternative possibility is that the mafic component is not mare basalt but a gabbronorite of nonmare affinity. Given the limited mineralogy of the lunar crust, the two possibilities cannot be easily distinguished on the basis of bulk composition. The single AN–MB glass for which we obtained SIMS data has REE concentrations very similar to those of the VLT basalt from NEA 003, however (Fig. 14).

The anorthosite norite component of Fig. 16 (Table 3) has the normative composition of 62 wt% plagioclase (~68 vol%), 6 wt% diopside, 23 wt% hypersthene, 7 wt% olivine, and 1 wt% ilmenite, with $Mg' = 66$. This mineralogy corresponds to a ferroan anorthositic norite (Stöffler et al., 1980). We are unaware of any samples in the Apollo collection that represent mixtures of anorthositic norite of nonmare affinity and either mare basalt or gabbronorite, although some lunar meteorites are similar in bulk composition and may represent such mixtures (Fig. 16; Korotev et al., 2009). There is no reason to expect that these impact glasses originated anywhere near the Apollo 16 site.

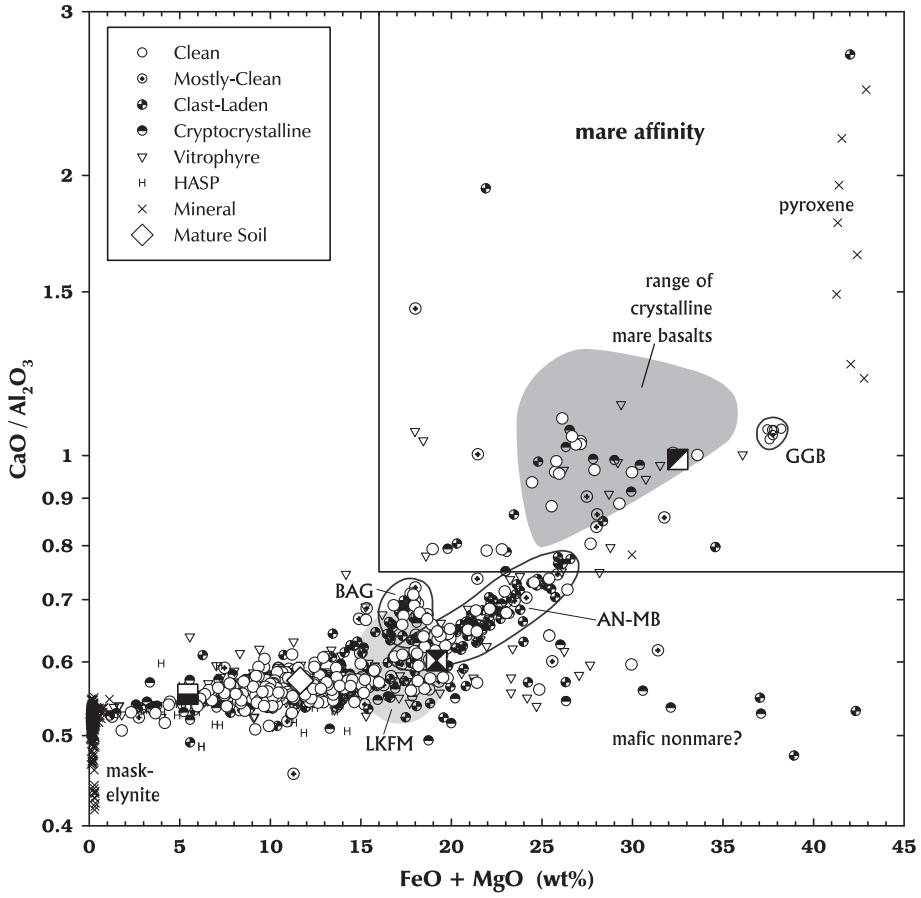

Fig. 15. A number of the impact glasses, 6.7%, are of mare affinity in having >16% FeO + MgO and CaO/Al_2O_3 >0.75. Of these, 21% have <1%, TiO_2, 54% have 1–6% TiO_2, and 25% have >6% TiO_2 (Fig. 9). Another 6.0% (AN–MB) have compositions intermediate to glass of anorthositic norite composition and mare basalt. The large squares represent the model components of Fig. 5. The lighter gray field represents the average composition of LKFM (low-K Fra Mauro basalt) glasses in Apollo 16 soil (±1 standard deviation ellipse) from Ridley et al. (1973). As in Figs. 8 and 9, the range of all known types of crystalline mare basalts is depicted. *Other acronyms:* BAG = basaltic andesite glass; GGB = green glass beads.

4.4. Comparison to impact melt splashes and bombs

In addition to glass fragments in the <1-mm fines, there are many samples of macroscopic (>1 cm^3) glass in the Apollo 16 collection that occur as "splashes" on rocks (Morris et al., 1986; See et al., 1986) and "bombs" in the regolith (Borchardt et al., 1986). Much of the macroscopic splash and bomb glass would fall into our clast-laden and cryptocrystalline categories; few would be clean. For example, See et al. (1986) state, "macroscopic analyses reveal that the [impact melt splashes] exhibit a glassy appearance, but the textures range from holohyaline to hyalopilitic. Schlieren-rich glasses dominate the holohyaline areas, and the crystalline areas are mainly spherulitic." The splash and bomb glass is characterized by the presence of FeNi metal and high concentrations of siderophile elements (e.g., 750 μg/g mean Ni). Spherules of similar composition up to 3 mm in diameter occur in the Apollo 16 regolith (Fig. 20).

Like the submillimeter impact glass in the regolith, the macroscopic impact glasses vary greatly in composition. Unlike the submillimeter glass, however, their average compositions are similar to that of the surface soil (Fig. 21). Many to most of the 50 glass splashes of Morris et al. (1986) are believed to have formed in the South Ray crater impact, which created a 0.7-km-diameter crater 6 km from station 1 (Morris et al., 1986). The 10 glass bombs of Borchardt et al. (1986) were all collected near 1-km-diameter North Ray Crater. Borchardt et al. (1986) argue that, in detail, these bombs are not soil melts, but melts of the subregolith basement by several impacts that formed craters less than 1.5 km in diameter. Thus, in terms of the discussion in the next section, we regard the splash and bomb glasses to have a local origin in that they are melts of lithologic components known to occur in the local Cayley and Descartes formations.

4.5. Local vs. nonlocal

We noted above that 65% of the clean impact glasses have compositions typical of or consistent with formation in the feldspathic highlands. However, many of these glasses differ in composition from the feldspathic highlands in the vicinity of the Apollo 16 site in three important ways.

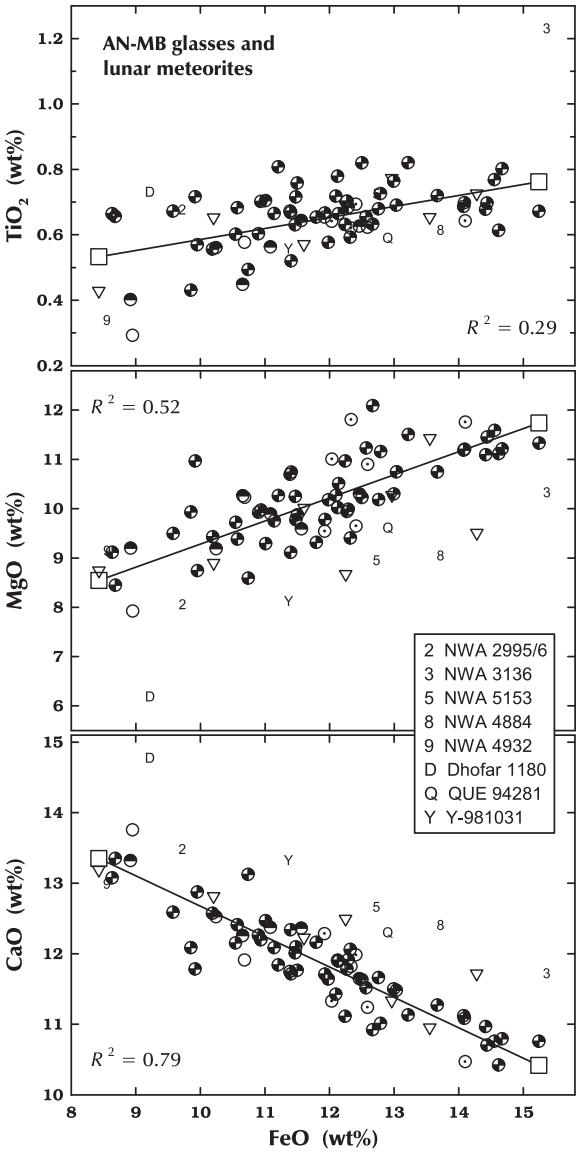

Fig. 16. Comparison of AN–MB glasses with lunar meteorites of similar composition. The lines are least-squares regressions to the glass data ($N = 69$) and the large squares represent the low-Fe and high-Fe compositions of Table 3. Most of the AN–MB glasses are cryptocrystalline (see legend in Fig. 7). Lunar meteorite data from Korotev et al. (2009) and sources therein. NWA 4932, QUE 94281, and Yamato 981031 probably all derive from the same source crater (Korotev et al., 2009).

The differences involve Mg', TiO_2, and incompatible elements. First, in the typical clean glass, FeO and MgO concentrations are 0.85× and 1.02× that of the Apollo 16 soil, leading to a mean Mg' of 70.1 ± 0.7 for the glass compared to 66.6 ± 0.2 for the soil (unless indicated otherwise, all uncertainties stated in this paper are 95% confidence limits). The data of Ridley et al. (1973) lead to essentially the same value of Mg', 70.3. It is clear from Fig. 10 that although many impact glasses have Mg' in the range of the soil, a number of others have very high Mg' compared typical rocks and soils of the feldspathic highlands. Some brecciated lunar meteorites have substantially greater Mg' than the Apollo 16 regolith, but several of the impact glasses have even greater values (Fig. 10). It is unlikely that high Mg' in the glass is caused mainly by fractional vaporization of Fe. An impact target with Apollo-16-soil composition would have to lose 65% of its iron to raise Mg' up to 85, for example. Under these circumstances, we would also expect substantial loss of silica (Fig. 6). However, the mean SiO_2 concentration of typical clean glasses with $Mg' > 80$ ($N = 15$) is 45.4 wt%, essentially the same as the soil, 45.0 wt% (Fig. 7). A possible contributing cause for a small portion of the Mg' difference is metal. Nine percent of the iron in typical Apollo 16 soil occurs as FeNi metal grains of meteoritic origin (Korotev, 1987; Table 5). We observed metal in some of the impact glasses but avoided it when choosing analytical points. The Mg' of the nonmetallic portion of the soil is 68.6, closer to the lean glass mean. Again, however, this explanation does not account for the high-Mg' glasses of Fig. 10. For the 15 otherwise "typical" glasses of Fig. 10 with $Mg' > 80$, the mean composition corresponds to 74.6% normative plagioclase ($An_{98.0}$), 2.0% diopside, 14.8% hypersthene, 7.7% olivine, 0.44% ilmenite, and 0.16% chromite, with Mg' averaging 84.5 for the mafic silicates. Glasses with even greater Mg', 90–98, have been identified in some Apollo 16 regolith breccias (Wentworth and McKay, 1988).

The second compositional difference is that concentrations of TiO_2 in the typical clean glass average $71 \pm 4\%$ of the concentration in the soil. The third difference is that concentrations Na_2O ($86 \pm 7\%$), K_2O ($50 \pm 5\%$) and P_2O_5 ($31 \pm 3\%$) are also significantly less in the glass than in Apollo 16 soil. We might reasonably assume that the depletions in Na, K, and P are the result of fractional vaporization (Fig. 6), except that the typical clean glasses are also low in Sm by the same factor as K_2O ($48 \pm 10\%$) despite the fact that Sm is much more refractory than K (Fig. 19). Most typical clean glasses have TiO_2, K_2O and Sm concentrations intermediate between those of the Apollo 16 regolith and the feldspathic lunar meteorites (Figs. 9, 19b). There is at most only a weak correlation between Mg' and K_2O concentration. The 139 typical clean glasses with $Mg' < 70$ have 0.065 ± 0.06 wt% K_2O whereas the 93 glasses with $Mg' > 70$ have only slightly less K_2O (0.051 ± 0.010 wt%). Only 38% of the "typical" (highlands) impact glass of Fig. 21 have Sm in the range of Apollo 16 soils and $Mg' < 70$. Only 13% of the glasses plot in the field of Apollo 16 soils in Fig. 21b, yet many of them plot in the range of lunar meteorites, most of which, because of their low concentrations of incompatible elements, must come from points distant from the Procellarum KREEP Terrane (Korotev et al., 2006). We take these various observation to indicate that much of the feldspathic impact glass of the Apollo 16 site was formed from target material like the source regions of the feldspathic lunar meteorites, that is, material less contaminated by KREEP than is the soil at the surface of the Apollo 16 site.

Earlier, we defined glass as atypical of the feldspathic highlands if it had >16 wt% FeO ± MgO, >1 wt% TiO_2, >0.2 wt% K_2O, or $Mg' < 50$ if both FeO and MgO are >2 wt%. If we consider all of the Apollo 16 impact (nonagglutinitic) glasses for which composition can provide some indication of place of origin (that is, excluding the

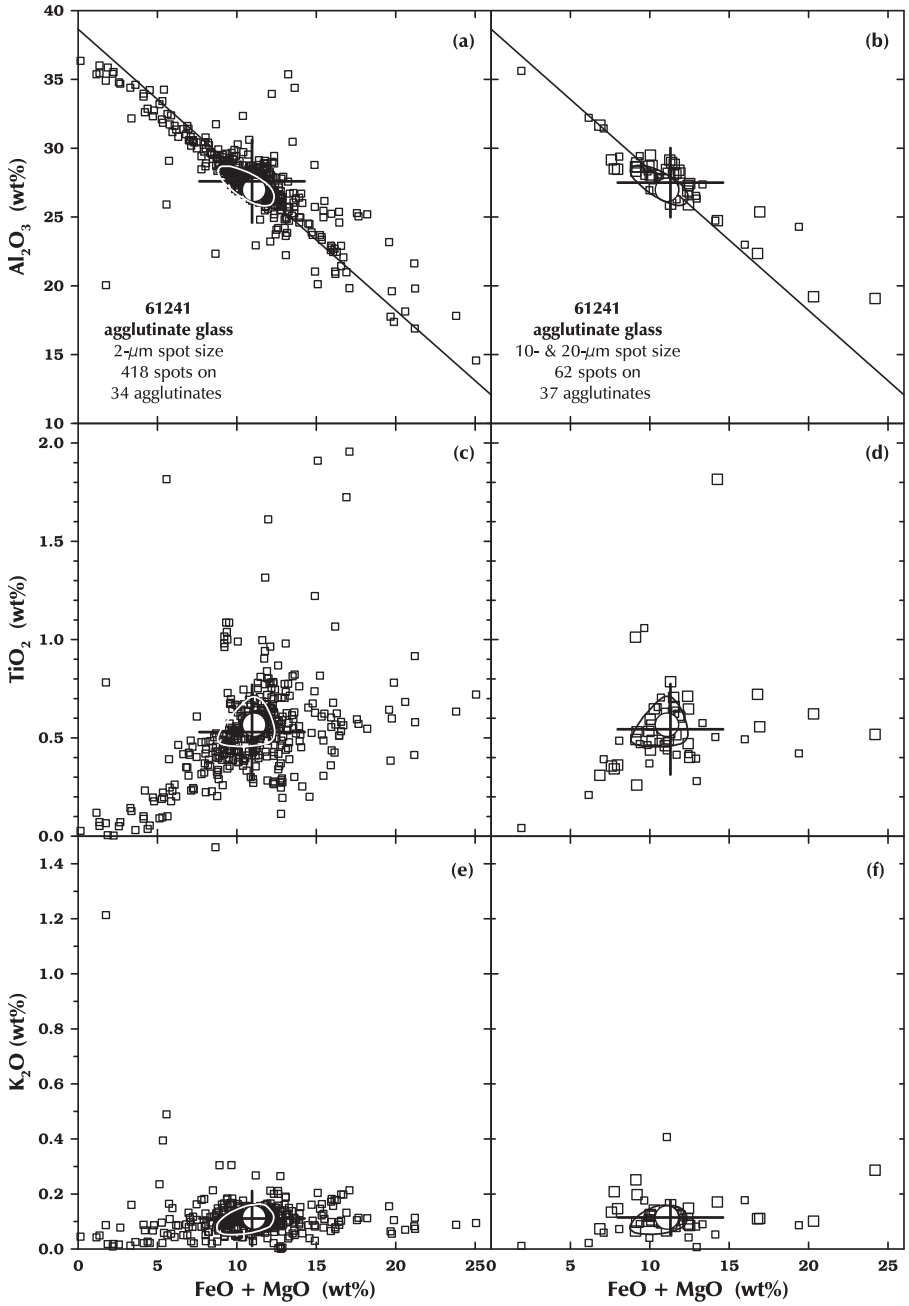

Fig. 17. Composition of glass in agglutinate fragments from sample 61241, EMPA data. Data on the right (b, d, and f) are from 37 fragments using a 10-μm spot for the 64–105-μm grain-size fraction (20 smaller squares) and a 20-μm-spot for the 105–210-μm fraction (17 larger squares). There are 1–4 analytical spots per fragment for a total of 62 spots. Data on the left (a, c, and e) are from 34 of the same 37 agglutinate fragments using a 2-μm beam spot size. All of the 2-μm spots were within the 10-μm or 20-μm spots. with an average of 12 2-μm spots per fragment for a total of 418 spots. In the 2-μm-spot data, the 21 high-TiO_2 points (>0.9%) are from 10 fragments. For three of the fragments, two or more spots are high in TiO_2. The six high-K_2O points (>0.3%) are from four fragments. The large + represents the mean and standard deviation of the agglutinitic glass compositions. In each plot the large white circle represents the mean composition of the seven soil samples (<1-mm fines) from station 1, where 61241 was collected (Table 1). The range is shown by the "ring (white on left, black on right). In (a) and (b), the diagonal line has no special significance with respect to the agglutinate data but is the same line as for the impact glasses of Fig. 8.

HASP glass and "mineral" glasses of Table 1), 40% are atypical of the feldspathic highlands. This value is somewhat greater than the 35% obtained above for the clean glasses because it includes the cryptocrystalline, vitrophyric, and clast-laden glasses.

If we further consider feldspathic glasses that are specifically atypical of Apollo 16, the proportions of glasses with exotic compositions increase. Mg' is consistently 65–67 in samples of mature Apollo 16 soil, yet for 34% of otherwise typical glasses, Mg' exceeds 70 (Fig. 10). (For this

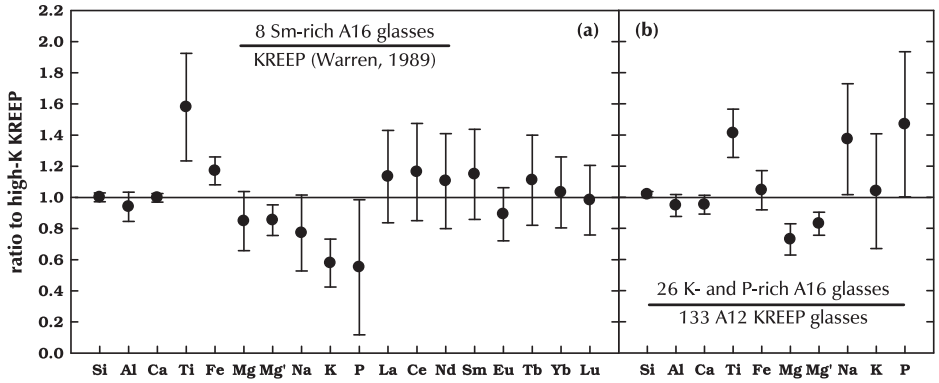

Fig. 18. Comparison of high-K, high-P glasses of this study to high-K KREEP samples of other sites. (a) For the eight most Sm-rich (>30 μg/g) glasses of Fig. 20 (all "clean" glasses with >30 μg/g Sm), average REE concentrations are in the range of Apollo-14-type high-K KREEP, a composition based mainly on rocks (Warren, 1989). The volatile, minor KREEP-related elements, Na, K, and P are low, however. The error bars are 95% confidence limits based on the data of the numerator. (b) Comparison of 26 glasses with >0.5% K_2O and >0.5% P_2O_5 (includes basaltic andesite glass) to high-K KREEP glass from Apollo 12 (based on means presented in the studies of Bunch et al. (1972), Englehardt et al. (1971), Meyer et al. (1971), Marvin et al. (1971), and Quaide et al. (1971)). The error bars are 95% confidence limits based on the data of both the numerator and denominator.

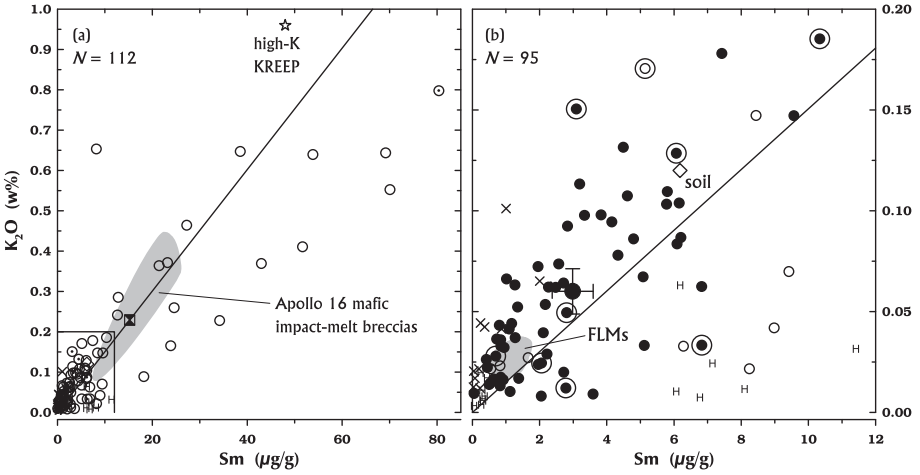

Fig. 19. K_2O and Sm concentrations (SIMS data) in all glasses for which SIMS data were obtained. Analytical uncertainties average 1% (K_2O) and 11% (Sm) of the concentration value. The diagonal line represents K_2O/Sm of Apollo 16 mafic, KREEP-bearing impact-melt breccia (hour glass in square, see text). (a) The range of the Apollo 16 KREEP-bearing, mafic impact-melt breccias is shown. The star represents the high-K KREEP composition (Apollo 14 mafic impact-melt breccias) of Warren (1989), which has greater K_2O/Sm than Apollo 16 KREEP. Several of the high-K, high-Sm glasses have low K_2O/Sm compared to KREEP. (b) Low-K, low-Sm portion of (a). Filled circles have major-element compositions typical of the feldspathic highlands. Unfilled circles represent glasses with compositions that are atypical of the feldspathic highlands; most are more mafic (>16% FeO + MgO; see text). Circled points fall in the LKFM range of Ridley et al. (1973). The large filled circle represents the mean of the typical points and the error bars represent the 95% confidence limits. This composition is more similar to the feldspathic lunar meteorites (FLMs) than it is to typical mature surface soil of Apollo 16 (diagonal square). The field for feldspathic lunar meteorites is defined by seven meteorites from Antarctica (Korotev et al., 2003). Most high-Sm HASP (high-alumina, silica-poor) glasses (H) are severely depleted in K compared to non-HASP glasses of similar Sm concentration. Maskelynite grains are depicted by ×.

calculation, we regard any glass having <2 wt% FeO or MgO as typical regardless of Mg'.) As noted earlier, the high Mg' is not the result of impact vaporization of iron because silica is not depleted. If we move all otherwise typical impact glasses with Mg' >70 to the atypical category, then the proportion of impact glasses atypical of Apollo 16 increases to 60%.

Of the 34 clean glasses with Apollo-16-soil-like major-elements concentrations by the tightened definition of the previous paragraph for which we measured Sm concentrations, 38% have FeO + MgO and Sm concentration lying outside the range of the Apollo 16 surface soils and impact melt splashes and bombs of Fig. 21. Most have Sm concentrations lower that that of Apollo 16 soils. If we assume the same proportion applies to all remaining impact glasses and move 38% of the remaining typical glasses to the atypical category, then 75% of the impact glass. This value provides an upper limit to the proportion of non-local glass fragments of ~0.1-mm grain size in the Apollo 16 regolith.

The logic we use above overestimates the proportion of non-local glass if some of the feldspathic, low-Sm glass was, in fact, formed locally, either from material below the

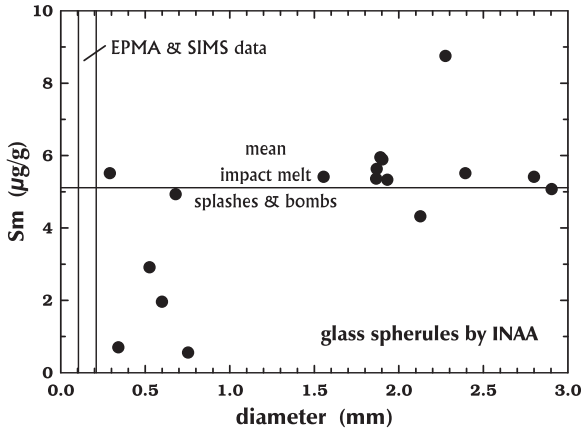

Fig. 20. Sm concentrations determined by instrumental neutron activation analysis on 17 individual glass spherules in the Apollo 16 regolith. The diameter was calculated from the analyzed mass assuming perfect spheres and a density of 2.7 g cm^{-3}. The data of Fig. 21 was taken on fragments in the "EPMA&SIMS" size range. All spherules greater than a millimeter in diameter lie in the range of the splashes and bombs of Fig. 21 (Morris et al., 1986; Borchardt et al., 1986) for all elements measured. Sm uncertainties are smaller than the points (2–5% of the concentration value).

Imbrium ejecta deposit upon which the Apollo 16 site is located (i.e., the Cayley Plains) or before admixture of Sm-rich material at the time of the Imbrium impact. The first scenario is unlikely because the data for the glass splashes and bombs, formed during local kilometer-sized crater impacts, are clearly rich in Sm (Fig. 21b) compared to most feldspathic lunar meteorites. The second scenario, pre-Imbrium impact glass, cannot be discounted. Wentworth and McKay (1988) report that 41% of the nonmare glass in Apollo 16 ancient regolith breccias is of "highland basalt" composition (Table 4). That composition (Table 4 of Wentworth and McKay (1988)) is indistinguishable from our typical clean glass composition (Table 3). The ancient regolith breccias were lithified about 4 billion years ago (McKay et al., 1986), thus glass of this composition has existed in the regolith since at least the time of the Imbrium impact. However, Wentworth and McKay (1988) also note that in the present soil, the relative proportion of feldspathic glass (highland basalt) is greater, 70% compared to the ancient regolith breccias, 41%. When the data of Delano et al. (2007) and this work are also taken into account, the proportion is 73% (Table 4). The difference (73% − 41%) suggests that since the time of closure of the ancient regolith breccias, presumably the time of basin formation, a significant amount of feldspathic impact glass has been added to the Apollo 16 regolith by small (1 km? 10 km?) impacts into the highlands. At a minimum, to simply raise the proportion of HB glass from 41% to 73% (Table 4) would require that 74% of the highland-basalt glass is post Imbrium. At a maximum, adding both LKFM and HB glass to the ancient regolith breccias to match relative proportions of the three glass types seen in the soil today (last row of Table 4) requires that 50% of the LKFM glass and 82% of the HB glass were added to the regolith after the closure of the ancient regolith breccias. These values are not unreasonable considering that virtually all of the glass that originates from mare targets is a post-basin additive (Zeigler et al., 2006). An additional consideration is that two Apollo 16 glasses of HB composition in the

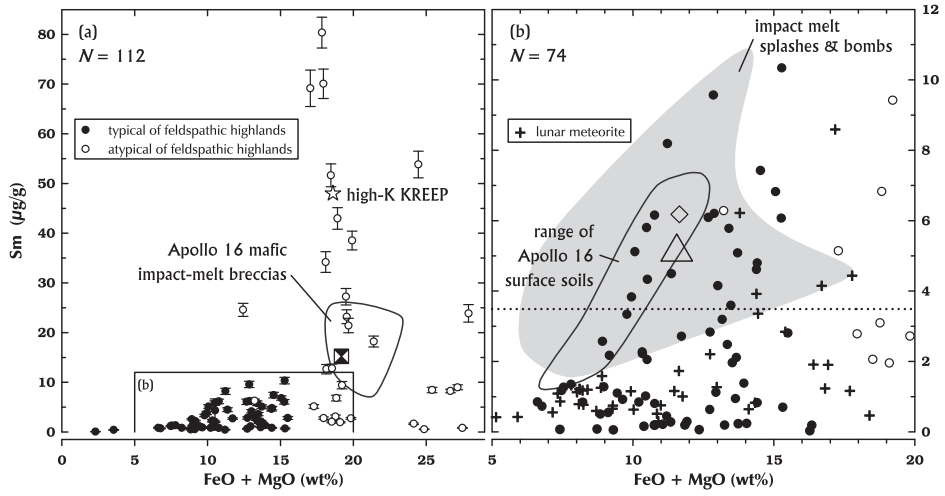

Fig. 21. Samarium concentrations in glasses for which SIMS data were obtained (circles). (a) Error bars represent analytical uncertainties (2σ). Among glasses with major-element compositions in the range of Apollo 14 (star, "high-K KREEP;" Warren, 1982) and Apollo 16 mafic impact-melt breccias, Sm concentrations vary greatly. (b) Portion of (a). As in other figures, the unfilled diagonal square represents the mean composition of mature surface soils (data sources given in Fig. 1). Also shown is the range of all 33 samples of Apollo 16 surface and trench soils for which data are available, which includes submature and immature soils (Fig. 1). Most fragments of impact glass with FeO + MgO concentrations in the range of the local soil have lower concentrations of Sm than the typical surface soil. The glasses also have lower concentrations of Sm than do the glassy melt splashes and bombs of Morris et al. (1986) and Borchardt et al. (1986); the large triangle represents the mean and the gray field represents the range of 60 samples. Many glasses, however, are in the range of the lunar meteorites (+). The dotted line represents the mean Sm concentration of the glasses (circles) in the figure (3.5 μg/g). Glass with <2 μg/g Sm would have <0.7 μg/g Th (Fig. 22).

Table 4
Percentage of compositional types of nonmare glass in ancient regolith breccias (ARBs) and the present soil of Apollo 16.

Glass from	KREEP	LKFM	HB	*N*	Source
ARBs	34.1	25.0	40.9	232	1
Soil	15.9	13.9	70.2	151	1
Soil	10.0	11.7	78.4	892	2
Soil	11.3	21.4	67.3	788	3
Soil	11.0	16.1	72.9	1831	1–3

KREEP, LKFM, and HB (highland basalt) classification from Table 2 of Wentworth and McKay (1988; *source 1*). *Source 2:* Delano et al. (2007). *Source 3:* this work. *N* is the total number of nonmare glasses analyzed.

study of Zellner et al. (2009) have formation ages of 983 ± 216 Ma (27.4 wt% Al_2O_3) and 805 ± 218 Ma (24.1 wt% Al_2O_3), much younger than the age of the Imbrium impact. Thus, we suspect that most impact glass in the Apollo 16 regolith was made by post-basin, crater-forming impacts.

If feldspathic glasses with, e.g., <2 μg/g Sm (equivalent to <0.7 μg/g Th; Fig. 21b) are not formed locally, then most must have formed hundreds of kilometers away (Fig. 22). Some, however, may have originated from the Kant Plateau, as close as 50 km east of the site (Andre and El-Baz, 1981).

4.6. Agglutinitic glass

The literature on the composition of agglutinitic glass is a minefield of apparent contradictions and inconsistencies. Intuition, as well as experimental data, suggests that a micrometeorite will locally melt what it strikes (Basu et al., 1996, 2002). If it happens to strike fine-grained regolith that is rich in solar-wind implanted gases, then an agglutinate with the composition of that regolith is produced and the glass in the agglutinate will have the same composition as the regolith, on average. At the opposite extreme, if a micrometeorite strikes a mineral grain or rock, the resulting glass will not have the composition of the local regolith, but it may also not have the vesicular morphology of an agglutinate if concentrations of solar-wind gases are low in the target.

In the 1970s several papers addressed the issue of whether agglutinates, or the glass in agglutinates, differ in composition from the regolith in which they were formed. In the first of these papers, Adams et al. (1975) and Rhodes et al. (1975) made magnetic separates of regolith and identified these as "agglutinate fractions." Their implicit assumption was that most of the metal in the regolith was or had been nanophase iron associated with regolith maturation and agglutinate formation. They observed that the "agglutinate fractions" were consistently richer in incompatible elements and elements associated with mafic minerals and depleted in elements associated with plagioclase compared to the bulk regolith. The effect was particularly strong in the Apollo 16 samples. Adams et al. (1975) and Rhodes et al. (1975) interpreted this result in terms of chemical fractionation associated with the formation of agglutinates by micrometeorite impacts, that is, that mafic phases

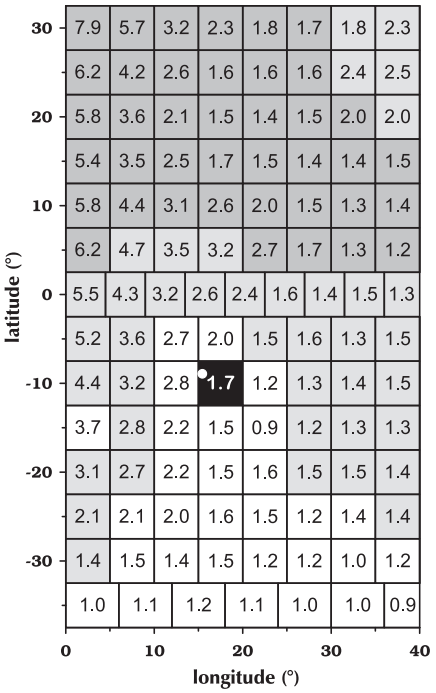

Fig. 22. Schematic map depicting surface concentrations of Th (in ppm = μg/g) in the vicinity of the Apollo 16 landing site (white circle in black square) as determined by Lunar Prospector (Prettyman et al., 2006). The 5-deg pixel containing the landing site yields 1.7 ppm Th, which compares with 2.2 ppm for typical mature Apollo 16 soil (Korotev, 1997). Pixels with darkest gray backgrounds have >24% FeO + MgO (Prettyman et al., 2006) and are in the maria (Figs. 8 and 9). Those with lighter gray backgrounds have 16–24% FeO + MgO. Only those with white backgrounds are in the feldspathic highlands (<16% FeO + MgO). Regionally, locations in the feldspathic highlands with low Th (and Sm; Fig. 19) occur in the Kant Plateau (squares to the immediate east and southeast of the site square). Near the landing site, 5° of latitude or longitude is ~150 km.

melted preferentially to plagioclase. As this work and numerous other works have shown, however, the composition of glass in agglutinates, although variable in composition, does not differ significantly, on average, from the composition of the regolith in which the agglutinates are formed (Marvin et al., 1971; Taylor et al., 1972; Gibbons et al., 1976; Via and Taylor, 1976; Hu and Taylor, 1977; Basu et al., 1996). The explanation for the data is that much of the metal in the lunar regolith, particularly regolith from the Apollo 16 site, is not associated with regolith maturation but rather derives from the mafic, metal-rich, KREEP-bearing, impact-melt breccias of which the regolith is in large part composed (20–25 wt% at Apollo 16). Such breccias contain 0.5–2 wt% FeNi metal. (Korotev, 1997). The magnetic separates may have been richer in agglutinates than the nonmagnetic separates, but they were certainly richer in the melt-breccia component (high FeNi metal, high Fe^{2+}, high REE) and poorer in metal-poor anorthosite than the bulk regolith. This hypothesis is essentially an extension of that of Via and Taylor (1976; "magnetic nonagglutinates").

The initial work on "agglutinate fractions" led to a lot of subsequent work on understanding agglutinate formation. For example, there is some evidence that the glass in agglutinates more closely reflects the composition of the <10-μm grain-size fraction than it does the <1-mm fraction (Walker and Papike, 1981; Taylor et al., 2001a,b, 2002). One explanation for the observation is that the finest material preferentially melts during micrometeorite impacts (Papike et al., 1981; Walker and Papike, 1981). However, large agglutinates in the 1–2-mm and 2–4-mm grain-size fractions of lunar regoliths have compositions that, on average, are indistinguishable from the regolith (<1-mm) in which they form (Blanchard et al., 1975; Jolliff et al., 1991, 1996). Little work has been done on the bulk composition of submillimeter agglutinates, where we might expect the largest differences between the compositions of agglutinates and the <1-mm regolith. One such work, that of Taylor et al. (1978) on ~100-μm agglutinates, does, in fact, demonstrate that the average composition of agglutinates can differ from that of the regolith (<1-mm) in which they are *found*. This work, however, concludes that agglutinates are redistributed by subsequent impacts and that they do, in fact, record the composition of the regolith in which they are *formed*. (The discussion of this and the previous paragraph is summarized from text the first author wrote for Lucey et al. (2006, p. 159).)

More recently, Taylor and colleagues have focused their efforts not on agglutinates, but on the glass in agglutinates – "agglutinitic glass" (Taylor et al., 2001a,b, 2002, 2003; Pieters and Taylor, 2003), the same type from which we obtained the data of Table 2 and Fig. 17. They make the intriguing observation that agglutinitic glass from Fe-rich, Al-poor mare regolith (Apollo 17) is more feldspathic (lower Fe, higher Al) than the bulk regolith whereas in Fe-poor, Al-rich highland regolith (Apollo 16), the agglutinitic glass is more mafic than the bulk regolith. Pieters and Taylor (2003) account for this observation with a two-part model. (1) A high proportion of the highland material in nominally mare regolith and a high proportion of the mare material in nominally highland regolith are in the form of impact glass redistributed over long distances. In Pieters and Taylor's (2003) words, "The suspected large scale mixing between mare and highlands is real, but contains a significant glass component." (2) During micrometeorite impacts into regolith, the pre-existing glass melts preferentially to the crystalline mineral components. The result is that agglutinitic glass from mafic regoliths such as that of Apollo 17 is more feldspathic than the soil (<1-mm fines) in which the agglutinates occur and, conversely, agglutinitic glass from feldspathic regoliths such as Apollo 16 is more mafic.

We concur with the first part of the model of Pieters and Taylor (2003). The nearside surface of the Moon is more mafic than the regolith of the Apollo 16 site because the rocks of the Apollo 16 site are mainly feldspathic yet vast exposures of mare basalt occur elsewhere. Maria exist within several hundred kilometers of the site in several directions (Fig. 22). Similarly, ballistically transported impact glass occurring in mare regolith will be more feldspathic, on average, than the regolith in which it is found because most of the Moon's surface is more feldspathic.

On the basis of the data of this work, however, we offer an alternate explanation for the observations leading to the second part of the model of Pieters and Taylor (2003). In essence, we suspect that a significant fraction of the glass identified by Taylor et al. (2001a,b, 2002, 2003) as "agglutinitic glass" is not, as they assume, glass derived from agglutinates but is impact glass from crater-forming events, which, at Apollo 16, is more mafic than true agglutinitic glass. We arrive at this conclusion for the following reasons. Taylor et al. (2001a) acknowledge that in fine grain-size fractions of the regolith they cannot distinguish agglutinitic glass on the basis of its most obvious physical characteristic, the presence of vesicles, because the glass fragments are small compared to the size of the vesicles. In Taylor et al. (2001b) they state that "all impact glasses are reported as agglutinitic glass because the compositions are identical" and "other nonagglutinitic, impact glasses actually make up only ≪10% of the amount measured." Neither statement is consistent with our data. (1) It is true that the composition of Apollo 16 glass identified as agglutinitic glass in the study of Taylor et al. (2003) is similar in composition to the impact glass of this study, but it is also considerably more mafic than the soil in which the agglutinates occur (Fig. 23). This latter observation is inconsistent with the data of Fig. 17 and several previous studies that

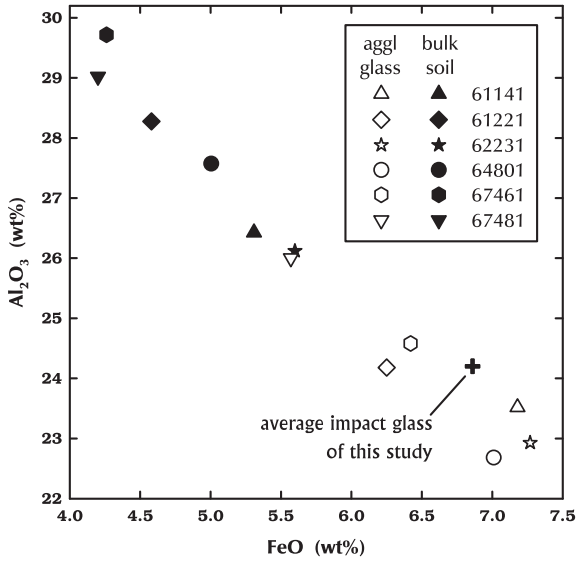

Fig. 23. Comparison of the (assumed average) compositions of "agglutinitic glass" from five Apollo 16 soils samples, as reported by Taylor et al. (2003), to the composition of the bulk soil (<1-mm fines) from which the agglutinates were separated. On average, the FeO concentration of the glasses are 37% greater that that of the corresponding soil, in contrast to the data of Fig. 17a, where there is virtually no difference. However, the non-agglutinitic impact glass of this study (Table 3) falls in the compositional range of the "agglutinitic glass" of Taylor et al. (2003). Soil data are averages calculated from data of Bansal et al. (1972), Duncan et al. (1973), Hubbard et al. (1973), Korotev, 1982, Laul and Papike (1980), Rose et al. (1973), Taylor et al. (1973), and Wänke et al. (1973). Al_2O_3 concentration of 62231 estimated on the basis of the FeO concentration.

have shown that agglutinitic glass, on average, is very similar in composition to the soil (Marvin et al., 1971; Taylor et al., 1972; Gibbons et al., 1976; Hu and Taylor, 1977; Basu et al., 1996). (2) In the samples studied here, the fraction of all glass fragments (i.e., agglutinate plus impact glass) that are impact glasses is not insignificant, as Taylor et al. (2001b) imply. As this and previous studies advocate (Delano, 1991; Zeigler et al., 2006; Delano et al., 2007), a substantial portion of the glass in the Apollo 16 regolith does indeed derive from distant sources as a result of crater-forming impacts. On average, the impact glass fragments and agglutinates occur in volumetrically similar proportions in the regolith. The proportion of glass fragments that are impact glasses ranges from 68% in immature soil 61221 to 27% in mature soil 68841 (Table 1). Clearly, the proportion of impact glass decreases with maturity as the proportion of agglutinates increases. Nevertheless, we studied three samples with a mean I_s/FeO of 42 whereas Taylor et al. (2002, 2003) studied six Apollo 16 samples with a mean I_s/FeO of 49, so differences in maturity is not the cause discrepancy. The work of Taylor et al. (2002, 2003) was done on <45-μm grain-size fractions whereas our data are for the 64–210 μm grain-size fractions. We see no reason to expect, however, that glass from agglutinates preferentially concentrates in the finer grain-size fractions, compared to impact glass, during comminution of the soil by micrometeorite impacts. So, we can only conclude that the Apollo 16 "agglutinitic glass" of Taylor et al. (2002, 2003) is as mafic as it is because it includes a significant proportion of glass produced in crater-forming impacts. Thus, we see no evidence for preferential melting of glass over crystalline material in the agglutinate-forming process.

5. CONCLUSIONS

Glass of impact origin is ubiquitous in the lunar regolith. In the 64–210-μm grain-size fraction of the three Apollo 16 regolith samples studied here, the proportion of fragments (14%) that are glasses made in crater-forming impacts is comparable to the proportion (16%) made by micrometeorite impacts (agglutinates). Macroscopic (>1 cm) samples of glass known or strongly suspected to have formed in craters within a few kilometers of the Apollo 16 site have a range of compositions but are generally similar in composition to the Apollo 16 regolith or some mixture of the major rocks types occurring in the Apollo 16 regolith. As much as 75% of the impact glass in the 64–210-μm grain-size fraction, however, has compositions inconsistent with formation from the Apollo 16 regolith or the major lithologic components of the regolith (low-Sm feldspathic breccias and moderate-Sm noritic breccias). Forty percent of the impact glass is either considerably more mafic than typical material of the feldspathic highlands or is much richer in Ti, K, and P. Such glass must originate in the maria or the Procellarum KREEP Terrane. Few glasses have compositions in the range of the mafic, KREEP-bearing impact-melt breccias that are prevalent among rocks of the Apollo 16 collection and most of the glasses that are rich in K, REE, and P are dissimilar in major-element composition from rocks identified as KREEP from Apollo 12 and 14 in being relativity richer in TiO_2 and having lower Mg/Fe. Conversely, although most Apollo 16 glasses have feldspathic compositions that are generally like that of the local soil, many are distinct from the soil in having lower concentrations of TiO_2 and elements associated with KREEP and greater Mg/Fe. These glasses likely derive from elsewhere in the feldspathic highlands. Several compositional groupings of glass in the Apollo 16 regolith are distinct from any rock or mixture of rocks collected on the Apollo missions although one, the AN–MB (anorthositic norite–mare basalt) glass described here is similar to some moderately mafic lunar meteorites.

On average, glass in the Apollo 16 regolith that was produced in crater-forming impacts is more mafic (greater Fe/Al) than the regolith whereas glass in agglutinates has the same composition as the regolith. This observation is a simple consequence of the fact that agglutinates mainly derive from local micrometeorite impacts into the surface regolith whereas crater-forming impacts distribute glassy ejecta over distances of tens to hundreds of kilometers. Because the Moon's surface within several hundred kilometers of the Apollo 16 site is more mafic, on average, than the Apollo 16 regolith, the impact glass is also more mafic, on average.

A small fraction, about 3%, of the impact glass has been severely affected by differential volatilization, leading to the composition known as HASP (high-alumina, silica poor). Ratios of refractory elements in HASP glasses (Sc/Al, Sm/Al) are dissimilar to those of the local regolith, suggesting that most HASP glass is also of distant origin.

ACKNOWLEDGMENTS

This work was supported by NASA Grant NNG06GF67G. We thank Hiroshi Nagasawa for providing the glassed sample of JB-1, Bill Satterwhite for preparation of the thin sections, Alian Wang for Raman spectrometric analyses, and Larry Taylor for enlightening discussion and inspiration. We also thank Abhijit Basu, Christian Koeberl, and, particularly, John Delano for their reviews and data (Delano).

REFERENCES

Adams J. B., Charette M. P. and Rhodes J. M. (1975) Chemical fractionation of the lunar regolith by impact melting. *Science* **190**, 380–381.

Andre C. G. and El-Baz F. (1981) Regional chemical setting of the Apollo 16 landing site and the importance of the Kant Plateau. *Proc. 12th Lunar Planet. Sci. Conf., Part B*, 767–779.

Apollo Soil Survey (1971) Apollo 14: nature and origin of rock types in soil from the Fra Mauro Formation. *Earth Planet. Sci. Lett.* **12**, 49–54.

Bansal B. M., Church S. E., Gast P. W., Hubbard N. J., Rhodes J. M. and Wiesmann H. (1972) The chemical composition of soil from the Apollo 16 and Luna 20 sites. *Earth Planet. Sci. Lett.* **17**, 29–35.

Basu A. (2005) Nanophase Fe^0 in lunar soils. *J. Earth Syst. Sci.* **114**, 375–380.

Basu A., McKay D. S., Morris R. V. and Wentworth S. J. (1996) Anatomy of individual agglutinates from a highland soil. *Meteorit. Planet. Sci.* **31**, 777–782.

Basu A., Wentworth S. J. and McKay D. S. (2002) Heterogeneous agglutinitic glass and the fusion of the finest fraction (F^3) model. *Meteorit. Planet. Sci.* **37**, 1835–1842.

Blanchard D. P. and Budahn J. R. (1979) Remnants from the ancient lunar crust: Clasts from consortium breccia 73255. *Proc. 10th Lunar Planet. Sci. Conf.*, 803–816.

Blanchard D. P., Korotev R. L., Brannon J. C., Jacobs J. W., Haskin L. A., Reid A. M., Donaldson C. H. and Brown R. W. (1975) A geochemical and petrographic study of 1–2 mm fines from Apollo 17. *Proc. 6th Lunar Sci. Conf.*, 2321–2341.

Borchardt R., Stöffler D., Spettel B., Palme H., Wänke H., Wacker K. and Jessberger E. K. (1986) Composition, structure, and age of the Apollo 16 subregolith basement as deduced from the chemistry of post-Imbrium melt bombs. *Proc. 17th Lunar Planet. Sci. Conf., in J. Geophys. Res.* **91**, E43–E54.

Boschelli L. J. and McKay D. S. (1987) Differential volatilization of lunar impact glass using Rayleigh fractionation modeling. *Lunar Planet. Sci. XVIII*. Lunar Planet. Inst., Houston. #109–110 (abstr.).

Bunch T. E., Prinz M. and Keil K. (1972) *Electron microprobe analyses of lithic fragments and glasses from Apollo 12 lunar samples*. Spec. Publ. 4, UNM Institute of Meteoritics, 1–14.

Chao E. C. T., Boreman J. A., Minkin J. A., James O. B. and Desborough G. A. (1970) Lunar glasses of impact origin: Physical and chemical characteristics and geologic implications. *J. Geophys. Res.* **75**, 7445–7479.

Chao E. C. T., Best J. B. and Minkin J. A. (1972) Apollo 14 glasses of impact origin and their parent rock types. *Proc. 3rd Lunar Sci. Conf.*, 907–925.

Delano J. W. (1975) Petrology of the Apollo 16 mare component: Mare Nectaris. *Proc. 6th Lunar Sci. Conf.*, 15–47.

Delano J. W. (1991) Geochemical comparison of impact glasses from lunar meteorites ALHA81005 and MAC88105 and Apollo 16 regolith 64001. *Geochim. Cosmochim. Acta* **55**, 3019–3029.

Delano J. W., Lindsley D. H. and Rudowski R. (1981) Glasses of impact origin from Apollo 11, 12, 15, and 16: Evidence for fractional vaporization and mare/highland mixing. *Proc. 12th Lunar Planet. Sci. Conf., Part B*, 339–370.

Delano J. W., Zellner N. E. B., Barra F., Olson E., Swindle T. D., Tibbetts N. J. and Whittet D. C. B. (2007) An integrated approach to understanding Apollo 16 impact glasses: Chemistry, isotopes, and shape. *Meteorit. Planet. Sci.* **42**, 993–1004.

Duncan A. R., Erlank A. J., Willis J. P. and Ahrens L. H. (1973) Composition and inter-relationships of some Apollo 16 samples. *Proc. 4th Lunar Sci. Conf.*, 1097–1113.

Engelhardt W. V., Arndt J., Müller W. F. and Stöffler D. (1971) Shock metamorphism and the origin of fines and breccias at the Apollo 11 and Apollo 12 sites. *Proc. 2nd Lunar Sci. Conf.*, 833–854.

Finkelman R. B., Baedecker P. A., Christian R. P., Berman S., Schnepfe M. M. and Rose, Jr., H. J. (1975) Trace-element chemistry and reducing capacity of size fractions from the Apollo 16 regolith. *Proc. 6th Lunar Sci. Conf.*, 1385–1398.

Floss C. (2000) Complexities on the acapulcoite–lodranite parent body: Evidence from trace element distributions in silicate minerals. *Meteorit. Planet. Sci.* **35**, 1073–1085.

Freeman J. J., Wang A., Kuebler K. E. and Haskin L. A. (2008) Characterization of natural feldspar by Raman spectroscopy for future planetary exploration. *Can. Mineral.* **46**, 1477–1500.

Gibbons R. V., Hörz F. and Schaal R. B. (1976) The chemistry of some individual lunar soil agglutinates. *Proc. 7th Lunar Sci. Conf.*, 405–422.

Glass B. P. (1971) Investigations of glass recovered from Apollo 12 sample 12057. *J. Geophys. Res.* **76**, 5649–5657.

Haloda J., Týcová P., Korotev R. L., Fernandes V. A., Burgess R., Thöni M., Jelenc M., Jakeš P., Gabzdyl P. and Košler J. (2009) Petrology, geochemistry, and age of low-Ti mare-basalt meteorite Northeast Africa 003-A: A possible member of the Apollo 15 mare basaltic suite. *Geochim. Cosmochim. Acta* **73**, 3450–3470.

Haskin L. A., Helmke P. A., Blanchard D. P., Jacobs J. W. and Telander K. (1973) Major and trace element abundances in samples from the lunar highlands. *Proc. 4th Lunar Sci. Conf.*, 1275–1296.

Heiken G. H., McKay D. S. and Fruland R. M. (1973) Apollo 16 soils: Grain size analyses and petrography. *Proc. 4th Lunar Sci. Conf.*, 251–265.

Houck K. J. (1982a) Petrologic variations in Apollo 16 surface soils. *Proc. 13th Lunar Planet. Sci. Conf., in J. Geophys. Res.* **88**, A197–A209.

Houck K. J. (1982b) Modal petrology of six soils from the Apollo 16 double drive tube core 64002. *Proc. 13th Lunar Planet. Sci. Conf., in J. Geophys. Res.* **88**, A210–A220.

Hsu W. (1995) *Ion microprobe studies of the petrogenesis of enstatite chondrites and eucrites*. Ph. D. Thesis, Washington University. 380 pp.

Hu H.-N. and Taylor L. A. (1977) Lack of chemical fractionation in major and minor elements during agglutinate formation. *Proc. 8th Lunar Sci. Conf.*, 3645–3656.

Hubbard N. J., Meyer, Jr., C., Gast P. W. and Wiesmann H. (1971) The composition and derivation of Apollo 12 soils. *Earth Planet. Sci. Lett.* **10**, 341–350.

Hubbard N. J., Rhodes J. M., Gast P. W., Bansal B. M., Shih C.-Y., Weismann H. and Nyquist L. E. (1973) Lunar rock types: The role of plagioclase in non-mare and highland rock types. *Proc. 4th Lunar Sci. Conf.*, 1297–1312.

Jolliff B. L., Korotev R. L. and Haskin L. A. (1991) Geochemistry of 2–4 mm particles from Apollo 14 soil (14161) and implications regarding igneous components and soil-forming processes. *Proc. Lunar Planet. Sci.* **21**, 193–219.

Jolliff B. L., Rockow K. M., Korotev R. L. and Haskin L. A. (1996) Lithologic distribution and geologic history of the Apollo 17 site: The record in soils and small rock particles from the highlands massifs. *Meteorit. Planet. Sci.* **31**, 116–145.

Jolliff B. L., Gillis J. J., Haskin L. A., Korotev R. L. and Wieczorek M. A. (2000) Major lunar crustal terranes: Surface expressions and crust-mantle origins. *J. Geophys. Res.* **105**, 4197–4416.

Kempa M. J. and Papike J. J. (1980) The Apollo 16 regolith: Comparative petrology of the >20 μm and 20–10 μm soil fractions, lateral transport and differential volatilization. *Proc. 11th Lunar Planet. Sci. Conf.*, 1635–1661.

Korotev R. L. (1982) Comparative geochemistry of Apollo 16 surface soils and samples from cores 64002 and 60002 through 60007. *Proc. 13th Lunar Planet. Sci. Conf., in J. Geophys. Res.* **87**, A269–A278.

Korotev R. L. (1987) The nature of the meteoritic components of Apollo 16 soil, as inferred from correlations of iron, cobalt, iridium, and gold with nickel. *Proc. 17th Lunar Planet. Sci. Conf., in J. Geophys. Res.* **92**, E447–E461.

Korotev R. L. (1991) Geochemical stratigraphy of two regolith cores from the central highlands of the Moon. *Proc. Lunar Planet. Sci. Conf.*. **21**, 229–289.

Korotev R. L. (1996) On the relationship between the Apollo 16 ancient regolith breccias and feldspathic fragmental breccias, and the composition of the prebasin crust in the Central Highlands of the Moon. *Meteorit. Planet. Sci.* **31**, 403–412.

Korotev R. L. (1997) Some things we can infer about the Moon from the composition of the Apollo 16 regolith. *Meteorit. Planet. Sci.* **32**, 447–478.

Korotev R. L. (2000) The great lunar hot spot and the composition and origin of the Apollo mafic ("LKFM") impact-melt breccias. *J. Geophys. Res.* **105**, 4317–4345.

Korotev R. L. (2005) Lunar geochemistry as told by lunar meteorites. *Chem. Erde* **65**, 297–346.

Korotev R. L., Morris R. V. and Lauer, Jr., H. V. (1984) Stratigraphy and geochemistry of the Stone Mountain core (64001/2). *Proc. 15th Lunar Planet. Sci. Conf., in J. Geophys. Res.* **89**, C143–C160.

Korotev R. L., Jolliff B. L., Zeigler R. A., Gillis J. J. and Haskin L. A. (2003) Feldspathic lunar meteorites and their implications for compositional remote sensing of the lunar surface and the composition of the lunar crust. *Geochim. Cosmochim. Acta* **67**, 4895–4923.

Korotev R. L., Zeigler R. A. and Jolliff B. L. (2006) Feldspathic lunar meteorites Pecora Escarpment 02007 and Dhofar 489: Contamination of the surface of the lunar highlands by post-basin impacts. *Geochim. Cosmochim. Acta* **70**, 5935–5956.

Korotev R. L., Zeigler R. A., Jolliff B. L., Irving A. J. and Bunch T. E. (2009) Compositional and lithological diversity among brecciated lunar meteorites of intermediate iron composition. *Meteorit. Planet. Sci.* **44**, 1287–1322.

Kurasawa H. (1968) A new silicate rock standard, JB-1 issued from the Geological Survey of Japan. *Geochem. J.* **2**, 185.

Laul J. C. and Papike J. J. (1980) The lunar regolith: Comparative chemistry of the Apollo sites. *Proc. 11th Lunar Planet. Sci. Conf.*, 1307–1340.

Lindstrom D. J., Wentworth S. J., Martinez R. R. and McKay D. S. (1994) Trace element identification of three chemically distinct very low titanium (VLT) basalt glasses from Apollo 17. *Geochim. Cosmochim. Acta* **58**, 1367–1375.

Lucey P., Korotev R. L., Gillis J. J., Taylor L. A., Lawrence D., Elphic R., Feldman B., Hood L. L., Hunten D., Mendillo M., Noble S., Papike J. J. and Reedy R. C. (2006) Chapter 2. Understanding the lunar surface and space–moon interactions. In *New Views of the Moon. Reviews in Mineralogy and Geochemistry*, vol. 60 (eds. B. L. Jolliff, M. A. Wieczorek, C. K. Shearer and C. R. Neal). Mineralogical Society of America, Washington, DC. pp. 83–219.

Marvin U. B., Wood J. A., Taylor G. J., Reid, Jr., J. B., Powell B. N., Dickey, Jr., J. S. and Bower J. F. (1971) Relative proportions and probable sources of rock fragments in the Apollo 12 samples. *Proc. 2nd Lunar Sci. Conf.*, 679–699.

McKay D. S., Fruland R. M. and Heiken G. H. (1974) Grain size and the evolution of lunar soil. *Proc. 5th Lunar Sci. Conf.*, 887–906.

McKay D. S., Bogard D. D., Morris R. V., Korotev R. L., Johnson P. and Wentworth S. J. (1986) Apollo 16 regolith breccias: Characterization and evidence for early formation in the mega-regolith. *Proc. 16th Lunar Planet. Sci. Conf., in J. Geophys. Res.* **91**(B4), D277–D303.

McKay D. S., Heiken G., Basu A., Blanford G., Simon S., Reedy R., French B. M. and Papike J. (1991) The lunar regolith. In *Lunar Sourcebook* (ed. G. Heiken et al.), Cambridge Univ. Press. Chapter 7, pp. 285–356.

Meyer, Jr., C. (1978) Ion microprobe analyses of aluminous lunar glasses: A test of the "rock type" hypothesis. *Proc. 9th Lunar Sci. Conf.*, 1551–1570.

Meyer, Jr., C., Brett R., Hubbard N. J., Morrison D. A., McKay D. S., Aitken F. K., Takeda H. and Schonfeld E. (1971) Mineralogy, chemistry, and origin of the KREEP component in soil samples from the Ocean of Storms. *Proc. 2nd Lunar Sci. Conf.*, 393–411.

Morris R. V. (1976) Surface exposure indices of lunar soils: A comparative FMR study. *Proc. 7th Lunar Sci. Conf.*, 315–335.

Morris R. V. (1978) The surface exposure (maturity) of lunar soils: Some concepts and I_s/FeO compilation. *Proc. 9th Lunar Planet. Sci. Conf.*, 2287–2297.

Morris R. V., See T. H. and Hörz F. (1986) Composition of the Cayley Formation at Apollo 16 as inferred from impact melt splashes. *Proc. 17th Lunar Planet Sci. Conf., in J. Geophys. Res.* **91**, E21–E42.

Müller O. (1975) Lithophile trace and major elements in Apollo 16 and 17 lunar samples. *Proc. 6th Lunar Sci. Conf.*, 1303–1311.

Naney M. T., Crowl D. M. and Papike J. J. (1976) The Apollo 16 drill core: Statistical analysis of glass chemistry and the characterization of a high alumina–silica poor (HASP) glass. *Proc. 7th Lunar Sci. Conf.*, 155–184.

Papike J. J., Simon S. B., White C. and Laul J. C. (1981) The relationship of the lunar regolith <10 μm fraction and agglutinates. Part I: A model for agglutinate formation and some indirect supportive evidence. *Proc. 12th Lunar Planet. Sci. Conf., Part B*, 409–420.

Papike J. J., Simon S. B. and Laul J. C. (1982) The lunar regolith: Chemistry, mineralogy, and petrology. *Rev. Geophys. Space Phys.* **20**, 761–826.

Pieters C. M. and Taylor L. A. (2003) Systematic global mixing and melting in lunar soil evolution. *Geophys. Res. Lett.* **30**, 2048. doi:10.1029/2003GL018212.

Prettyman T. H., Hagerty J. J., Elphic R. C., Feldman W. C., Lawrence D. J., McKinney G. W. and Vaniman D. T. (2006) Elemental composition of the lunar surface: Analysis of gamma ray spectroscopy data from Lunar Prospector. *J. Geophys. Res.* **111**(E12), E12007. doi:10.1029/2005JE002656.

Prinz M., Bunch T. E. and Keil K. (1971) Composition and origin of lithic fragments and glasses in Apollo 11 samples. *Contrib. Mineral. Petrol.* **32**, 211–230.

Quaide W., Oberbeck V., Bunch T. and Polowski G. (1971) Investigation of the natural history of the regolith at the Apollo 12 site. *Proc. 2nd Lunar Sci. Conf.*, 701–718.

Reid A. M., Warner J., Ridley W. I. and Brown R. W. (1972a) Major element composition of glasses in three Apollo 15 soils. *Meteoritics* **7**, 395–415.

Reid A. M., Ridley W. I., Harmon R. S., Warner J., Brett R., Jakeš P. and Brown R. W. (1972b) Highly aluminous glasses in lunar soils and the nature of the lunar highlands. *Geochim. Cosmochim. Acta* **36**, 903–912.

Reid A. M., Warner J., Ridley W. I. and Brown R. W. (1972c) Major element composition of glasses in three Apollo 15 soils. *Meteoritics* **7**, 395–415.

Reid A. M., Duncan A. R. and Richardson S. H. (1977) In search of LKFM. *Proc. 8th Lunar Sci. Conf.*, 2321–2338.

Rhodes J. M., Adams J. B., Blanchard D. P., Charette M. P., Rodgers K. V., Jacobs J. W., Brannon J. C. and Haskin L. A. (1975) Chemistry of agglutinate fractions in lunar soils. *Proc. 6th Lunar Sci. Conf.*, 2291–2307.

Ridley W. I., Reid A. M., Warner J. L., Brown R. W., Gooley R. and Donaldson C. (1973) Glass compositions in Apollo 16 soils 60501 and 61221. *Proc. 4th Lunar Sci. Conf.*, 309–321.

Rose, Jr., H. J., Cuttitta F., Berman S., Carron M. K., Christian R. P., Dwornik E. J., Greenland L. P. and Ligon, Jr., D. T. (1973) Compositional data for twenty-two Apollo 16 samples. *Proc. 4th Lunar Sci. Conf.*, 1149–1158.

Seddio S. M., Jolliff B. L., Korotev R. L. and Zeigler R. A. (2009) A newly characterized granite from the Apollo 12 regolith. *Lunar Planet. Sci. XL*. Lunar Planet. Inst., Houston. #2285 (abstr.).

See T. H., Horz F. and Morris R. V. (1986) Apollo 16 impact-melt splashes – Petrography and major-element composition. *Proc. 17th Lunar Planet. Sci. Conf., in J. Geophys. Res.* **91**, E3–E20.

Simon S. B., Papike J. J., Shearer C. K., Hughes S. S. and Schmitt R. A. (1989) Petrology of Apollo 14 regolith breccias and ion microprobe studies of glass beads. *Proc. 19th Lunar Planet. Sci. Conf.*, 1–17.

Stöffler D., Knöll H.-D., Marvin U. B., Simonds C. H. and Warren P. H. (1980) Recommended classification and nomenclature of

lunar highlands rocks – A committee report. In *Proc. Conf. Lunar Highlands Crust* (eds. J. J. Papike and R. B. Merrill). Pergamon Press. pp. 51–70.

Taylor G. J., Marvin U. B., Reid, Jr., J. B. and Wood J. A. (1972) Noritic fragments in the Apollo 14 and 12 soils and the origin of Oceanus Procellarum. *Proc. 3rd Lunar Sci. Conf.*, 995–1014.

Taylor S. R., Gorton M. P., Muir P., Nance W., Rudowski R. and Ware N. (1973) Lunar highlands composition: Apennine Front. *Proc. 4th Lunar Sci. Conf.*, 1445–1459.

Taylor G. J., Wentworth S., Warner R. D., Keil, K. (1978) Agglutinates as recorders of fossil soil compositions. *Proc. 9th Lunar Sci. Conf.*, 1959–1967.

Taylor L. A., Pieters C. M., Keller L. P., Morris R. V., McKay D. S., Patchen A. and Wentworth S. (2001a) The effects of space weathering on Apollo 17 soils: Petrographic and chemical characterization. *Meteorit. Planet. Sci.* **36**, 285–299.

Taylor L. A., Pieters C. M., Keller L. P., Morris R. V. and McKay D. S. (2001b) Lunar mare soils: Space weathering and the major effects of surface-correlated nanophase Fe. *J. Geophys. Res.* **106**, 27,985–27,999.

Taylor L. A, Morris R. V, Pieters C, Patchen A., Taylor D.-H., Keller L. P. and McKay D. S (2002) Moon-wide evidence that the fusion-of-the-finest fraction – F^3 – model really explains the chemistry of the agglutinitic glass. *Lunar Planet. Sci. XXXIII*. Lunar Planet. Inst., Houston. #1291 (abstr.).

Taylor L. A., Pieters C., Patchen A., Taylor D.-H., Morris R. V., Keller L. P. and McKay D. S. (2003) Mineralogical characterization of lunar highland soils. *Lunar Planet. Sci. XXXIV*. Lunar Planet. Inst., Houston. #1774 (abstr.).

Vaniman D. T. and Papike J. J. (1980) Lunar highland melt rocks: Chemistry, petrology, and silicate mineralogy. In *Proc. Conf. Lunar Highlands Crust* (eds. J. J. Papike and R. B. Merrill). Pergamon, New York. pp. 271–337.

Via W. N. and Taylor L. A. (1976) Chemical aspects of agglutinate formation: Relationships between agglutinate composition and composition of the bulk soil. *Proc. 7th Lunar Sci. Conf.*, 393–402.

Walker R. J. and Papike J. J. (1981) The relationship of the lunar regolith <10 μm fraction and agglutinates. Part II: Chemical composition of agglutinate glass as a test of the "fusion of the finest fraction" (F^3) model. *Proc. 12th Lunar Planet. Sci. Conf., Part B*, 421–432.

Wänke H., Baddenhausen H., Dreibus G., Jagoutz E., Kruse H., Palme H., Spettel B. and Teschke F. (1973) Multielement analyses of Apollo 15, 16, and 17 samples and the bulk composition of the Moon. *Proc. 4th Lunar Sci. Conf.*, 1461–1481.

Warren P. H. (1989) KREEP: Major-element diversity, trace-element uniformity (almost). In *Workshop on Moon in Transition: Apollo 14, KREEP, and Evolved Lunar Rocks* (eds. G. J. Taylor and P. H. Warren). LPI Tech. Rpt. 89-03. Lunar and Planetary Institute, Houston. pp. 149–153.

Warren P. H., Taylor G. J., Keil K., Kallemeyn G. W., Shirley D. N. and Wasson J. T. (1983) Seventh foray: Whitlockite-rich lithologies, a diopside-bearing troctolitic anorthosite, ferroan anorthosites, and KREEP. *Proc. 14th Lunar Planet. Sci. Conf., in J. Geophys. Res.* **88**, B151–B164.

Wentworth S. J. and McKay D. S. (1988) Glasses in ancient and young Apollo 16 regolith breccias: Populations and ultra Mǵ glass. *Proc. 18th Lunar Planet. Sci. Conf.*, 67–77.

Wentworth S., Taylor G. J., Warner R. D., Keil K., Ma M.-S. and Schmitt R. A. (1979) The unique nature of Apollo 17 VLT basalts. *Proc. 10th Lunar Planet. Sci. Conf.*, 207–223.

Wentworth S. J., McKay D. S., Lindstrom D. J., Basu A., Martinez R. R., Bogard D. D. and Garrison D. H. (1994) Apollo 12 ropy glasses revisited. *Meteoritics* **29**, 323–333.

Zeigler R. A., Korotev R. L., Jolliff B. L., Haskin L. A. and Floss C. (2006) The geochemistry and provenance of Apollo 16 mafic glasses. *Geochim. Cosmochim. Acta* **70**, 6050–6067.

Zeigler R. A., Korotev R. L. and Jolliff B. L. (2007) Petrography, geochemistry, and pairing relationships of basaltic lunar meteorite stones NWA 773, NWA 2700, NWA 2727, NWA 2977, and NWA 3160. *Lunar Planet. Sci. XXXVIII*. Lunar Planet. Inst., Houston. #2109 (abstr.).

Zellner N. E. B., Spudis P. D., Delano J. W., Whittet D. C. B. (2002) Impact glasses from the Apollo 14 landing site and implications for regional geology. *J. Geophys. Res.* **107**(E11), 5102-12, doi: 1029/2001JE001800.

Zellner N. E. B., Delano J. W., Swindle T. D., Barra F., Olsen E. and Whittet D. C. B. (2009) Evidence from $^{40}Ar/^{39}Ar$ ages of lunar impact glasses for an increase in the impact rate 800 Ma ago. *Geochim. Cosmochim. Acta* **73**, 4590–4597.

Zinner E. and Crozaz G. (1986a) A method for the quantitative measurement of rare earth elements by ion microprobe. *Int. J. Mass Spectrom. Ion Processes* **69**, 17–38.

Zinner E. and Crozaz G. (1986b) Ion probe determination of the abundances of all the rare earth elements in single mineral grains. In *Secondary Ion Mass Spectrometry, SIMS V* (eds. A. Benninghoven, R. J. Colton, D. S. Simons and H. W. Werner). Springer-Verlag, New York. pp. 444–446.

Associate editor: Christian Koeberl